

Inhibitors of Tumor Progression Loci-2 (Tpl2) Kinase and Tumor Necrosis Factor α (TNF- α) Production: Selectivity and in Vivo Antiinflammatory Activity of Novel 8-Substituted-4-anilino-6-aminoquinoline-3-carbonitriles

Neal Green,^{*,†} Yonghan Hu,[†] Kristin Janz,[†] Huan-Qiu Li,[†] Neelu Kaila,[†] Satenig Guler,[†] Jennifer Thomason,[†] Diane Joseph-McCarthy,[†] Steve Y. Tam,[†] Rajeev Hotchandani,[†] Junjun Wu,[†] Adrian Huang,[†] Qin Wang,[‡] Louis Leung,[‡] Jefferey Pelker,[§] Suzana Marusic,[§] Sang Hsu,[§] Jean-Baptiste Telliez,[§] J. Perry Hall,[§] John W. Cuzzo,^{§,#} and Lih-Ling Lin[§]

Chemical and Screening Sciences, Wyeth Research, 200 Cambridge Park Drive, Cambridge, Massachusetts 02140, Drug Safety and Metabolism and Pharmacokinetics, Wyeth Research, Building G, Andover, Massachusetts, and Collegeville, Pennsylvania, and Inflammation Signaling, Wyeth Research, 200 Cambridge Park Drive, Cambridge, Massachusetts 02140

Received April 12, 2007

Tumor progression loci-2 (Tpl2) (Cot/MAP3K8) is a serine/threonine kinase in the MAP3K family directly upstream of MEK. Recent studies using Tpl2 knockout mice have indicated an important role for Tpl2 in the lipopolysaccharide (LPS) induced production of tumor necrosis factor α (TNF- α) and other proinflammatory cytokines involved in diseases such as rheumatoid arthritis. Initial 4-anilino-6-aminoquinoline-3-carbonitrile leads showed poor selectivity for Tpl2 over epidermal growth factor receptor (EGFR) kinase. Using molecular modeling and crystallographic data of the EGFR kinase domain with and without an EGFR kinase-specific 4-anilinoquinazoline inhibitor (erlotinib, Tarceva), we hypothesized that we could diminish the inhibition of EGFR kinase by substitution at the C-8 position of our 4-anilino-6-aminoquinoline-3-carbonitrile leads. The 8-substituted-4-anilino-6-aminoquinoline-3-carbonitriles were prepared from the appropriate 2-substituted 4-nitroanilines. Modifications to the C-6 and C-8 positions led to the identification of compounds with increased inhibition of TNF- α release from LPS-stimulated rat and human blood, and these analogues were also highly selective for Tpl2 kinase over EGFR kinase. Further structure–activity based modifications led to the identification of 8-bromo-4-(3-chloro-4-fluorophenylamino)-6-[(1-methyl-1H-imidazol-4-yl)methylamino]quinoline-3-carbonitrile, which demonstrated in vitro as well as in vivo efficacy in inhibition of LPS-induced TNF- α production.

Introduction

Inflammatory cytokines such as tumor necrosis factor α (TNF- α) and interleukin-1 (IL-1) are believed to be major contributors to inflammatory diseases such as psoriasis, Alzheimer's disease, inflammatory bowel disease, and most notably rheumatoid arthritis (RA).^{1–3} RA is a debilitating systemic disease that affects over 1% of the population worldwide with an annual incidence of 0.04%.³ The disease is characterized by recurring symptoms such as pain, swelling, stiffness, and restricted mobility due to the erosion of joint cartilage, connective tissue, and eventually bone. Furthermore, several mechanisms may contribute to the pathology of RA, adding to the complex treatment of this disease. TNF- α contributes to cartilage breakdown and bone erosion by stimulating the production of other proinflammatory cytokines such as IL-1 and IL-6 and inducing degradative enzymes such as the matrix metalloproteases (MMPs).^{1,4} Disease-modifying antirheumatic drugs that target TNF- α and IL-1 including etanercept (Enbrel), infliximab (Remicade), and adalimumab (Humira) have shown efficacy in the treatment of RA. Routes of administration, contraindications, and/or precautions associated with these agents warrant further investigation toward additional drug therapies.^{5,6}

Several pharmaceutical companies have focused on TNF- α converting enzyme (TACE) for the treatment of inflammatory diseases.⁴ Candidates such as BMS-561392 and TMI-1 (**3**) have shown efficacy in animal models of arthritis and have advanced to clinical trials; however, safety and efficacy concerns eventually led to their discontinuation (Chart 1).⁵

An alternative method toward the inhibition of TNF- α production is through disruption of signal transduction pathways that include several members of the mitogen activated protein kinase (MAP kinase) family, particularly p38 kinase. The identification of the inhibitor SB203580 initiated intense focus in the pharmaceutical industry for the discovery of p38 inhibitors.⁷ Compounds such as VX-745 (Vertex Pharmaceuticals), BIRB-796 (Boehringer-Ingelheim), and AMG-548 (Amgen; see Chart 1) represent the first examples of small-molecule p38 kinase inhibitors to advance into the clinic.⁸ In addition, GlaxoSmithKline, Roche, Scios, Pfizer, and Array BioPharma have also advanced p38 kinase inhibitors to the clinic for RA and other inflammatory diseases.⁹

Upstream activation of the MAP kinases is controlled by tumor progression loci-2 (Tpl2) kinase, a serine/threonine kinase in the MAP3K family.^{10–12} Recent studies using Tpl2 knockout mice confirmed that Tpl2 plays an important role in the lipopolysaccharide (LPS) induced production of TNF- α and other proinflammatory cytokines.¹³ Tpl2 is also required for TNF- α -induced signaling, and thus, an inhibitor of Tpl2 may provide multiple benefits by blocking both TNF- α production and signaling.^{14–17} Tpl2 is not inhibited by staurosporine, a nonspecific kinase inhibitor, and it is the only known human kinase that has a proline instead of a conserved glycine in the

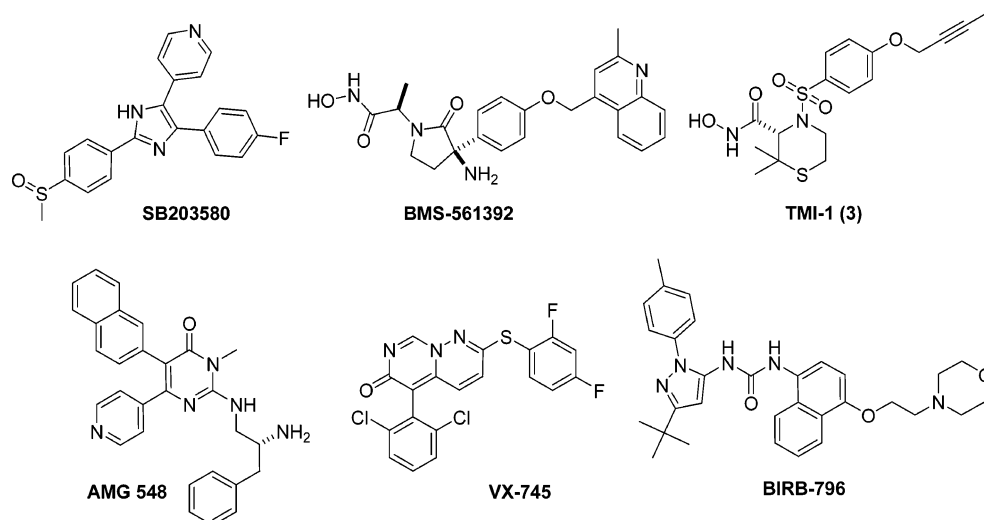
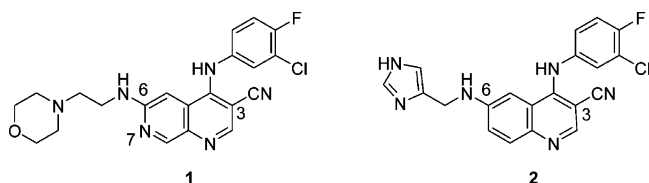
* To whom correspondence should be addressed. Phone: (617) 665-5604. Fax: (617) 665-5682. E-mail: ngreen@wyeth.com.

[†] Chemical and Screening Sciences.

[‡] Drug Safety and Metabolism and Pharmacokinetics.

[§] Inflammation Signaling.

[#] Present address: Praecis Pharmaceuticals, 830 Winter Street, Waltham, MA 02451.

Chart 1. Chemical Structures of TACE and p38 Kinase Inhibitors of TNF- α Production**Chart 2.** 1,7-Naphthyridine-3-carbonitrile (**1**) and Quinoline-3-carbonitrile (**2**) Inhibitors of Tpl2

glycine-rich ATP binding loop, a factor that may lead to the discovery of highly selective inhibitors.¹⁷

We have previously disclosed a series of 1,7-naphthyridine-3-carbonitriles (**1**) and more recently the related quinoline-3-carbonitrile (cyanoquinoline) Tpl2 inhibitors (**2**, Chart 2).^{18,19} Both of these leads were identified from our in-house kinase inhibitor collection, which comprises mostly tyrosine kinase inhibitors. Initial selectivity for Tpl2 over other kinases, particularly epidermal growth factor receptor (EGFR) tyrosine kinase, was moderate to poor for both the 1,7-naphthyridine-3-carbonitriles and cyanoquinolines. In this report we describe our efforts toward improving selectivity and potency of the cyanoquinoline class of Tpl2 inhibitors.²⁰

Design and Synthesis

The synthesis of most of the cyanoquinoline analogues with variations at X and at R started with the substituted nitroanilines **4a–g** (Scheme 1).²¹ Nitroanilines **4b–g** were reacted with ethyl 2-cyano-3-ethoxyacrylate under basic conditions to give the 2-cyano-3-(arylamino)acrylates **5b–g**.¹⁹ The acrylates were washed liberally with water upon workup and then dried in a vacuum oven for 48 h prior to thermal cyclization in Dowtherm A, which provided quinolones **6b–f** in moderate to good yields. The fluoroquinolone **6b** was converted to a thioether with sodium methylthiolate in 1,3-dimethyltetrahydropyrimidinone (DMPU) at room temperature²² and subsequently oxidized with either 1.2 or 2.2 equiv of *m*-chloroperbenzoic acid (*m*-CPBA) to provide the sulfoxide **6h** and the sulfone **6i**, respectively.²³ After chlorination of **6b–i**, the 3-fluoro-4-chloroaniline headpiece was installed by S_NAr displacement to give nitro intermediates **8b–i**. Demethylation of **8f** with pyridinium hydrochloride in DMF gave the corresponding –OH derivative **8j**.²⁴ Reduction of **8b–j** using tin dichloride²⁵ or catalytic hydrogenation²⁶ afforded the C-6 amino compounds **9b–j**. Attachment of moieties onto the C-6 amino group (tailpieces)

was accomplished by reductive amination²⁷ using a variety of commercially available or readily synthesized aldehydes to provide target 4-anilino-6-aminoquinoline-3-carbonitrile analogues **10–18**, **24–28**, **31–37**, **42–51**, and **55** (see Tables 1–3).

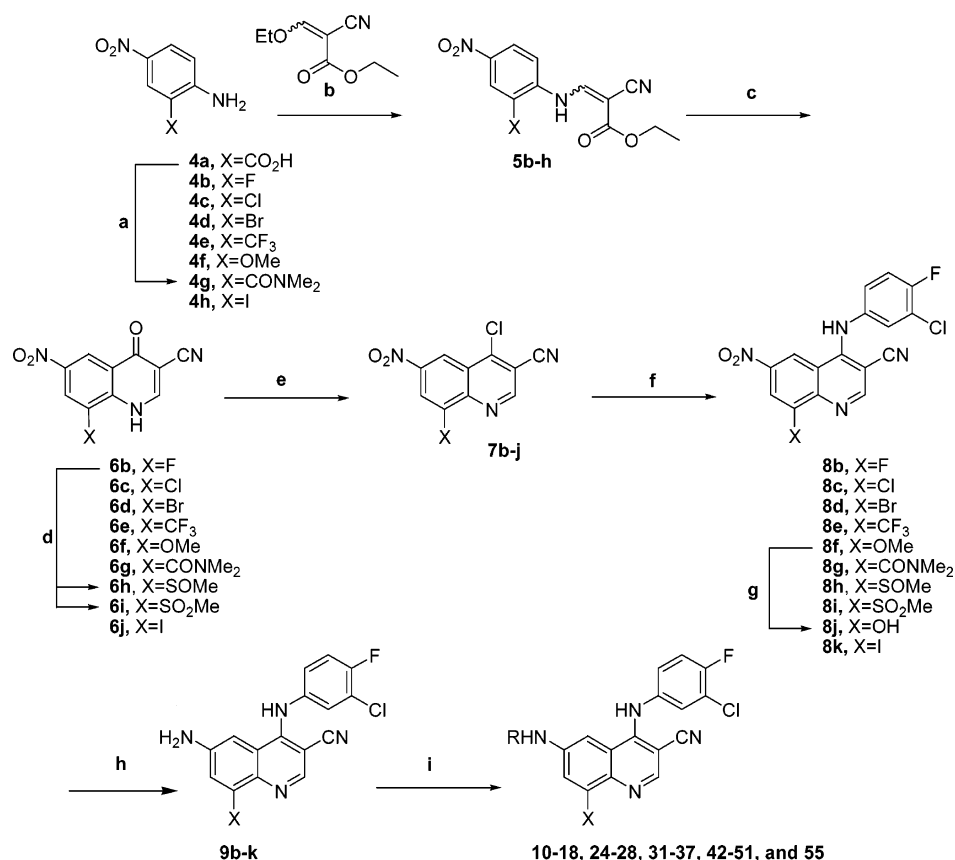
The synthesis of C-8 substituted analogues **19–21** was accomplished according to the chemistry shown in Scheme 2. Iodide **9n** was subjected to a Stille coupling reaction with tributyl(1-ethoxyvinyl)stannane, and the resulting enol ether was hydrolyzed to give **19**. Alkylation of **9d** gave **9l**, which was acetylated, subjected to dihydroxylation, and deprotected to give the dihydroxy intermediate **9m**. Reductive amination of **9m** afforded analogue **20**. Alkylation of the hydroxyl group of **8j** gave the *O*-allyl intermediate **8l**, and reduction of the nitro group and subsequent reductive amination gave **21**.

The syntheses of compounds **22**, **23**, **29**, **30**, and **38–41**, all of which include substituted imidazolyl and pyridinyl tailpieces, are shown in Schemes 3 and 4. A microwave-assisted Wittig homologation²⁸ of trityl-protected 1*H*-imidazole-5-carbaldehyde afforded 2-(1*H*-imidazol-5-yl)acetaldehyde, which was used in a reductive amination reaction with **9d** to give **22**. Acylation of **9d** with imidazolylacetic acid provided **23**. A bromine–magnesium exchange with 3,5-dibromopyridine²⁹ was used to furnish the pyridylaldehydes for the preparation of **29** and **30**. The method of Paul et al. (Scheme 4) was used to prepare **52–54**, leading to the quinolinecarbonitriles **38–41**.³⁰ A Sonogashira coupling reaction followed by reduction of the resulting alkyne and reductive amination was used to convert **56**³¹ to **43**.

Discussion

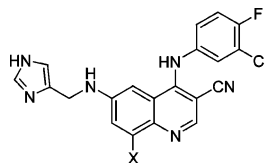
Molecular Modeling. We had previously studied the structure–activity relationships of a series of cyanoquinolines and found that potency improvement was afforded by variation of the 6-amino tailpiece portion while substitution at other sites on the scaffold ablated Tpl2 inhibition.¹⁹ In that report it was shown that compound **2** was a potent inhibitor of Tpl2 kinase with an IC₅₀ value of 30 nM but that it was equally potent against EGFR kinase. Our initial plan was to improve selectivity and potency through variation of the C-4 headpiece moiety;³² however, SAR studies of related 1,7-naphthyridine-3-carbonitriles did not show this approach to be effective.¹⁸

At the early stages of this project the low yield for the expression of Tpl2 and the difficulty in isolating stable and active protein deterred efforts toward X-ray crystallographic studies with this kinase. In addition, no suitable homology model

Scheme 1^a

^a Conditions: (a) BOP, 4-methylmorpholine, Me₂NH₂HCl, CH₂Cl₂, 100%; (b) Cs₂CO₃, DMF, room temp, 2 h, 72–99%; (c) Dowtherm A, 259 °C, 4–5 h, 21–68%; (d) (i) MeSNa, DMPU, room temp, 38%, (ii) MCPBA, CH₂Cl₂, room temp, 3 or 16 h; (e) (COCl)₂, DMF (cat.), DCE or POCl₃, reflux, 12 h, 85–92%; (f) 3-fluoro-4-chloroaniline, EtOH, reflux, 12 h, 41–78%; or DME, 120 °C microwave, 15 min; (g) pyridine·HCl, pyridine, 110 °C; (h) SnCl₄·2H₂O, EtOH, reflux 1 h or microwave, 110 °C, 5 min, or Pd/C, H₂, EtOH, acetic acid, 12 h, 63–90%; (i) RCHO, NaCNBH₃, HOAc, EtOH or DCE, Na(OAc)₃BH, 3 h, 4–76%.

Table 1. Tpl2 and P-EGFR Inhibition SAR



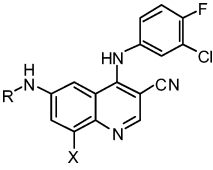
compd	X	IC ₅₀ (nM) ^a		LPS induced TNF-α inhibition ^b	
		Tpl2	P-EGFR	monocytes (nM)	human blood (nM)
2	H	20	30	600	3300
10	F	20	500	510	>10000
11	Cl	20	1800	350	4900
12	Br	10	3300	370	>10000
13	CF ₃	160	>20000	600	>10000
14	OH	11300	NT ^c	NT ^c	NT ^c
15	OMe	130	2080	3000	>10000
16	SOMe	20	5000	2130	13300
17	SO ₂ Me	190	NT ^c	NT ^c	NT ^c
18	CONMe ₂	130	>20000	>1000	>10000
19	C(O)Me	23	156	580	>10000
20	CH ₂ CH(OH)CH ₂ OH	910	NT ^c	NT ^c	NT ^c
21	OCH ₂ CH(OH)CH ₂ OH	830	NT ^c	NT ^c	NT ^c

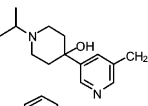
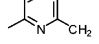
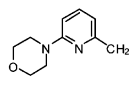
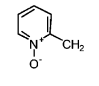
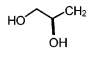
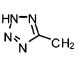
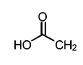
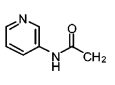
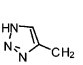
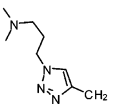
^a Average of at least two runs performed in duplicate with a standard deviation of 20%. ^b Average of at least two runs performed in duplicate with a standard deviation of 25%. ^c NT: not tested.

for Tpl2 was found that could be used for inhibitor–protein docking studies. In order to improve selectivity against EGFR, we used molecular modeling and the crystal structure of the EGFR kinase domain with a 4-anilinoquinazolinone inhibitor³³ (erlotinib) to determine an alternative site on our cyanoquinoline core.³⁴ Thus, the sequences of human EGFR and Tpl2 were

aligned and sequence differences were examined. The following residue differences were observed near the ATP binding site (numbering according to the EGFR structure, EGFR/Tpl2): Met⁷⁴²/Cys, Cys⁷⁵¹/Ala, Thr⁷⁶⁶/Met, Leu⁷⁶⁸/Ala, Met⁷⁶⁹/Gly, Pro⁷⁷⁰/Glu, and Thr⁸³⁰/Val. Two residues in particular, Leu⁷⁶⁸ (Ala in Tpl2) and Pro⁷⁷⁰ (Glu in Tpl2), are in the hinge region

Table 2. SAR of Various Tailpiece Analogues



compound	X	Tpl2 (enzyme) IC ₅₀ (nM) ^a	LPS induced TNF-α inhibition ^b monocytes	human blood (nM)	P-EGFR IC ₅₀ (nM) ^a	compound	R	X	Tpl2 (enzyme) IC ₅₀ (nM) ^a	LPS induced TNF-α inhibition ^b monocytes	human blood (nM)	P-EGFR IC ₅₀ (nM) ^a
11	Cl	20	350	4900	1800	30		Cl	500			
12	Br	10	370	>10,000	3300	31		Cl	170			
22	Cl	130		>20,000		32		Cl	350			
23	Br	>5000				33		Cl	18	1500	11,400	2900
24	Cl	290				34		Br	590			
25	Br	98	665	>20,000		35		Cl	2	>5000	>20,000	
26	Br	250				36		Cl	200	>5000	>20,000	
27	Cl	280				37		Cl	110			
28	Cl	16	>1000	>20,000	>5000	51		Br	18	74	3500	>5000
29	Cl	>3000				55		Br	20	221	3080	>5000

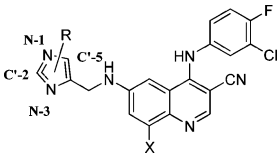
^a Average of at least two runs performed in duplicate with a standard deviation of 20%. ^b Average of at least two runs performed in duplicate with a standard deviation of 25%.

and are the only side chain differences near the C-8 position of erlotinib in the X-ray complex structure. Glide XP^{38,39} was used to dock compound **2** into the binding site of EGFR, and the predicted location of C-8 in the cyanoquinoline inhibitors was shown to overlay with the C-8 position in erlotinib (see Figure 1). Maps of preferred functional group positions within the unliganded EGFR binding site were calculated using MCSS;^{40,41} these calculations indicate that a methyl or larger group attached at C-8 to erlotinib or our cyanoquinoline inhibitors would be expected to have substantial steric clash with the hinge residues in EGFR. It is clear from Figure 1 that a methyl in an optimal position near the hinge residues (shown in cyan) is far too close to be bonded to erlotinib or the cyanoquinoline inhibitor **2** without shifting the inhibitor scaffold out of the pocket somewhat and thereby reducing EGFR inhibition. It was also predicted that substitution at the C-8 position of a cyanoquinoline would have a negligible impact on its binding to Tpl2 because the Leu⁷⁶⁸ in EGFR is replaced by the much smaller Ala side chain in Tpl2, allowing for larger substituents in this area. We did not know with certainty what the three-dimensional similarities were between EGFR kinase and Tpl2 kinase; therefore, we prepared a number of C-8 substituted cyanoquinolines in order to determine what groups would provide detrimental binding to EGFR kinase but maintain or improve Tpl2 inhibition.

Structure–Activity Relationships (SAR). All compounds were examined for inhibition of isolated Tpl2 enzyme via

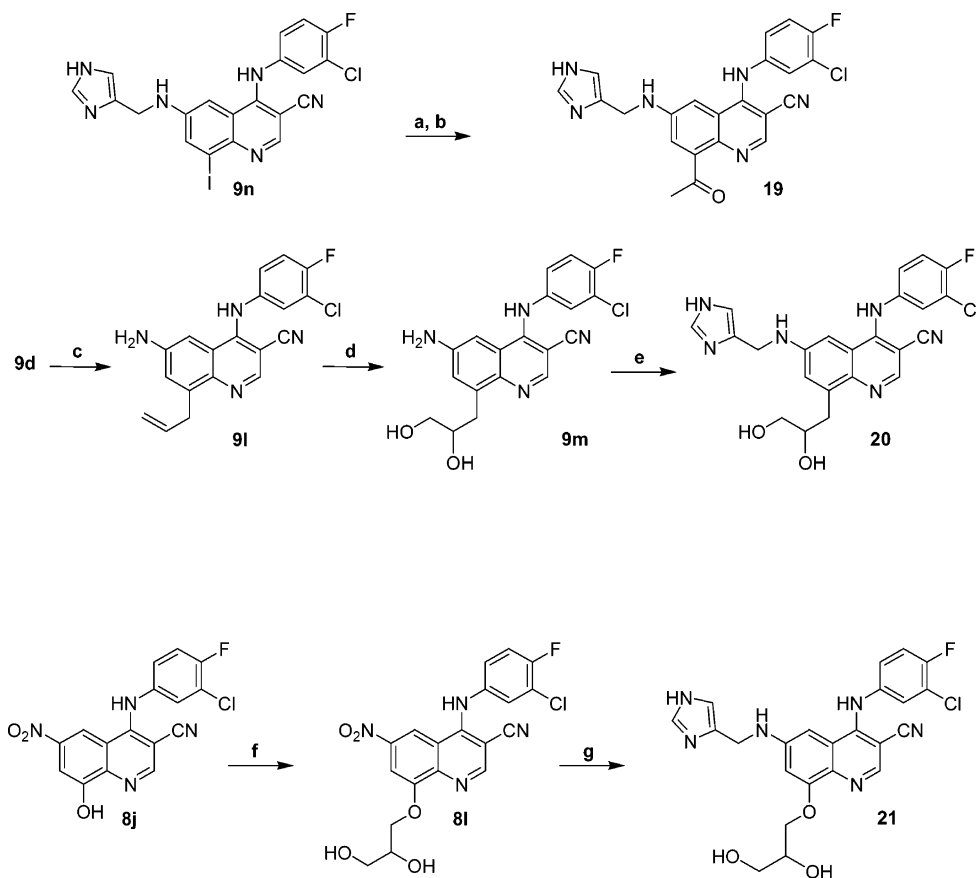
quantification of MEK phosphorylation in an ELISA format.^{18,19} For several compounds, selectivity was measured against EGFR kinase autophosphorylation in A431 cells overexpressing this enzyme.²¹ Functional inhibition of TNF-α production was measured using LPS-stimulated monocytes and LPS-stimulated human blood. Compounds studied in vivo were first assessed for selectivity against other kinases (including p38α, CAMKII, PKC, PKA, MK2, Src, S6K, IKKβ, and Jnk-1).

Our first goal was to study the impact that C-8 substitution would have on potency and selectivity. Toward that end, we chose groups with a range of sizes and polarity and the ability to donate and/or accept a hydrogen bond. We also attempted to make a possible contact with the ribose-binding region of Tpl2 with diols **19–21**. We were pleased to find that for **10**, **11**, and **12** (X = F, Cl, and Br, respectively) not only was potency maintained but more importantly a significant improvement in selectivity (25- to 470-fold) was demonstrated. The potency against Tpl2 was lower for nonhalogenated C-8 compounds **13–15** and **17**. Larger polarizable groups (Cl, Br, SOMe) appear to be favored for both Tpl2 inhibition and EGFR selectivity. A C-8 methyl group appears to be less favored by Tpl2, perhaps because simple van der Waals interactions in the absence of other electronic contributions are detrimental to binding. For example, a cyanoquinoline with a methyl group at C-8 and a 3-pyridyl in place of the imidazole tailpiece (not shown) had a Tpl2 kinase inhibition IC₅₀ of >1 μM. Other halogen C-8

Table 3. SAR and TNF- α Inhibition of Substituted Imidazole Tailpiece Analogues


compd	R	X	Tpl2 (enzyme) IC ₅₀ (nM) ^a	LPS induced TNF- α inhibition ^b	
				monocytes (nM)	human blood (nM)
11	H	Cl	20	580	5200
12	H	Br	10	320	11600
38	C'5-isopropyl	Br	130	2200	>20000
39	C'5-isopropyl	Cl	16	NT ^c	5800
40	C'5-propyl	Cl	25	220	5600
41	C'5-ethyl	Cl	16	NT ^c	7500
42	C'5-CO ₂ Me	Br	87	2000	>20000
43	C'5-[3-(dimethylamino)propyl]	Cl	130	NT ^c	15200
44	N'1-methyl	Br	30	670	6300
45	C'2-ethyl-C'5-methyl	Cl	320	NT ^c	NT ^c
46	C'2,5-dimethyl	Cl	220	NT ^c	NT ^c
47	N'3-methyl	Cl	220	NT ^c	>20000
48	C'2-phenyl	Br	5900	NT ^c	NT ^c
49	N'1-[2-(morpholinyl)ethyl]	Br	41	430	8950
50	N'1-[2-(methylsulfonyl)ethyl]	Br	43	1000	>20000

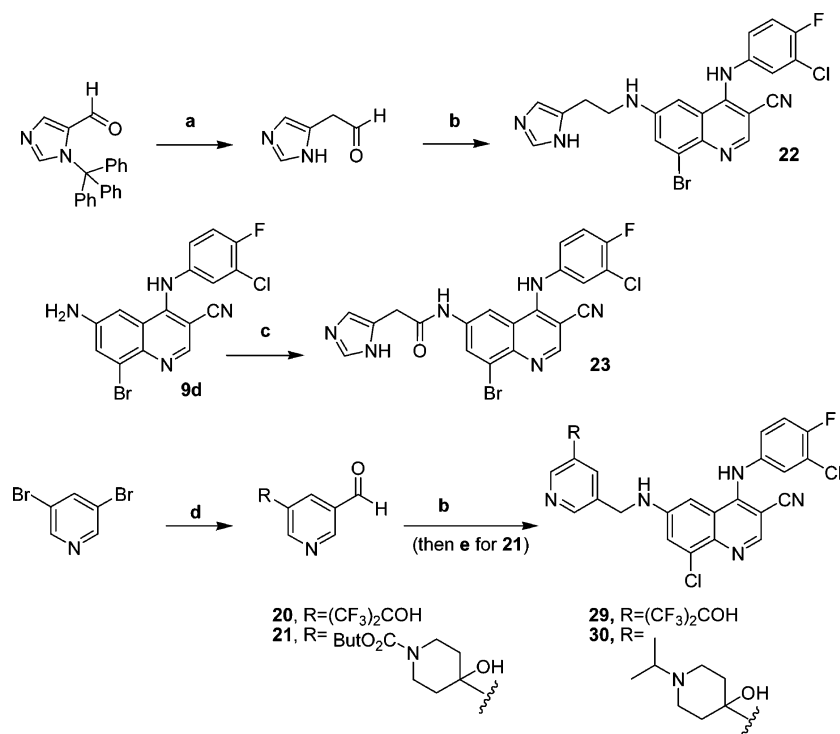
^a Average of at least two runs performed in duplicate with a standard deviation of 20%. ^b Average of at least two runs performed in duplicate with a standard deviation of 25%. ^c NT: not tested.

Scheme 2^a

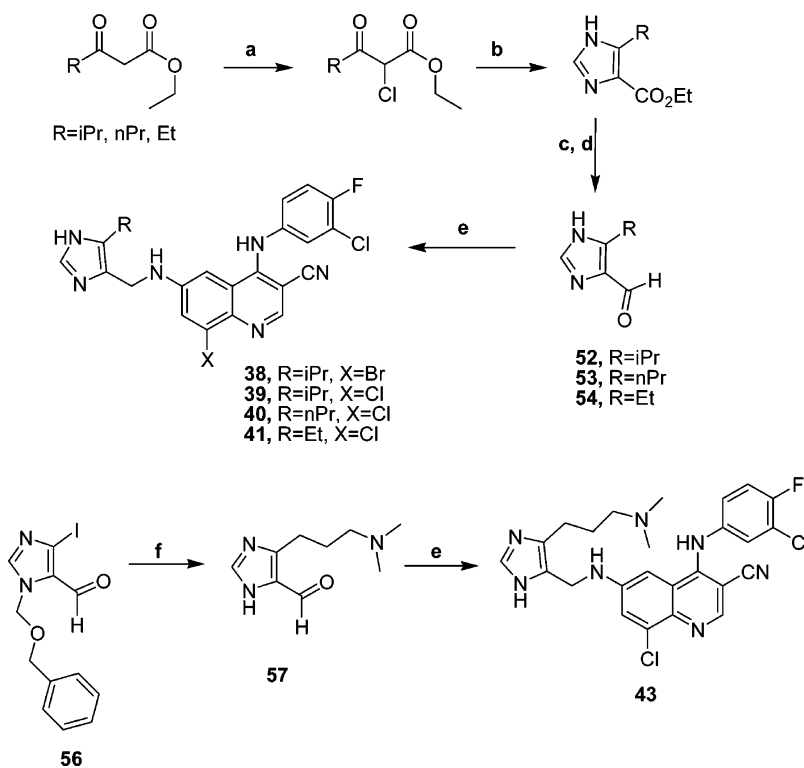
^a Conditions: (a) tributyl(1-ethoxyvinyl)tin, PdCl₂(PPh₃)₂, DMF; (b) 1 N HCl, heat, 14%; (c) allyltributylstannane, PdCl₂(PPh₃)₂, DMF, 48%; (d) (i) (CF₃CO)₂O, pyridine, CH₂Cl₂; (ii) OsO₄, NMO, acetone/H₂O, 1:1; (iii) 5 M LiOH, quantitative; (e) 1H-imidazole-5-carbaldehyde, HOAc, EtOH, Na(OAc)₃BH, 45%; (f) (i) allyl bromide, K₂CO₃, DMF, 75%; (ii) OsO₄, NMO, acetone/H₂O, 47%; (g) (i) SnCl₂·2H₂O, EtOAc; (ii) 1H-imidazole-5-carbaldehyde, HOAc, EtOH, Na(OAc)₃BH, 54%.

substitutions with this same tailpiece (e.g., compound **28**, Table 2) showed potency similar to that of the imidazole-substituted compounds.

The lack of Tpl2 potency for **14** and moderate potency for the corresponding methyl ether **15** indicated that a hydrogen bond donor group at the C-8 position was not tolerated. An

Scheme 3^a

^a Conditions: (a) (i) (methoxymethyl)triphenylphosphonium bromide, NaH, THF; (ii) MeOH, THF, HCl; (b) **9d**, THF, DMF, NaCNBH₃, HOAc, 22–50%; (c) 2-(1*H*-imidazol-5-yl)acetic acid, BOP, NMM, DMF; (d) (i) *i*-PrMgCl, THF, hexafluoroacetone, or *i*-PrMgCl, THF, *tert*-butyl 4-oxopiperidine-1-carboxylate; (ii) *i*-PrMgCl, THF, DMF, 19–22%; (e) (i) TFA, CH₂Cl₂ (1:3), 2 h, 100%; (ii) acetone, THF, EtOH, NaCNBH₃ 90%.

Scheme 4^a

^a Conditions: (a) SO₂Cl₂, CHCl₃, 0 °C to reflux, 2 h, 94%; (b) formamide, H₂O, 5–30%; (c) (i) LAH, THF, 70–90%; (d) MnO₂, acetone–CH₂Cl₂, 30–50%; (e) **9c** or **9d**, THF, DMF, NaCNBH₃, HOAc, 30–55%; (f) (i) *N,N*-dimethylprop-2-yn-1-amine, PdCl₂(PPh₃)₂, DMF, 90 °C, 2.5 h; (ii) Pd/C, H₂, THF, 3 h; (iii) 6 N HCl, MeOH, reflux, 12 h.

interesting SAR result was seen with the sulfoxide **16** and the sulfone **17**: the sulfoxide was nearly 10-fold more potent. This may be attributed to a potential repulsive steric or electronic interaction in that binding region due to the additional oxygen

atom on the sulfone. Alternatively, or in addition to the lack of an additional oxygen atom, the sulfoxide must be capable of adapting a favorable conformation unavailable to the sulfone **17** or the amide **18**. The smaller ketone analogue **19** was

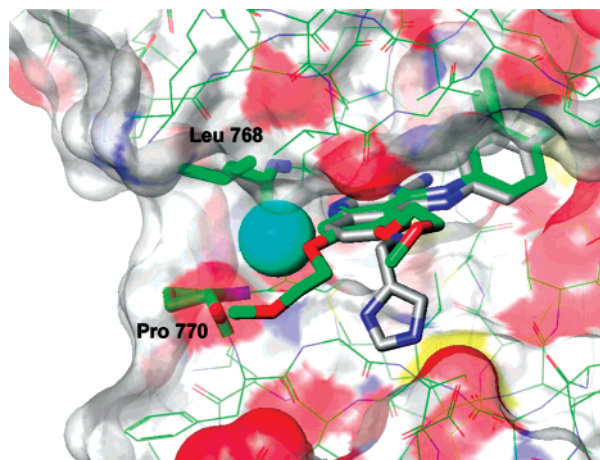


Figure 1. Structure of EGFR with erlotinib bound shown colored by element with carbons in green and a translucent molecular surface on the protein. A model of compound **2** bound to EGFR is also shown in thick lines colored by element with carbons in gray. A calculated optimal position for methyl in the binding site is shown in a space filling model in cyan. Glide XP^{38,39} (Schrodinger, Inc., New York, NY) was used to dock compound **2** into the unliganded binding site of EGFR, and MCSS^{40,41} was used to calculate optimal methyl positions in the binding site.

comparable in potency to the sulfoxide **16** but lacked the selectivity seen for the halogenated analogues. The diols **20** and **21** were also 10-fold less potent than **10–12**, which may be a result of negative steric interactions.

Having discovered that C-8 substitution with halogen maintained potency and improved selectivity, we varied the C-6 tailpiece portion of the cyanoquinoline scaffold in order to further improve enzymatic and cellular potency. In addition, we attempted to address the potential metabolic liability of compound **11**. In vitro metabolic studies with **11** indicated that the compound was moderately metabolized in rat ($t_{1/2} = 35$ min), mouse ($t_{1/2} = 23$ min), and human ($t_{1/2} = 31$ min) liver microsomes with N-dealkylation, desaturation, and hydroxylation being the major metabolic pathways (Figure 2). We therefore chose C-6 replacements with more sterically demanding groups, longer carbon tethers, or groups with different electronic properties to reduce the metabolism at this position.

As seen previously in studies with the related 1,7-naphthyridine-3-carbonitrile series¹⁸ and shown here in Table 2, enzymatic potency was sensitive to C-6 tailpiece changes. Compared with imidazole tailpiece analogue **11**, pyridyl **28** and pyridyl N-oxide **33** had similar enzymatic potencies while pyrazoles **24–26**, the imidazopyridine **27**, the diol **34**, the carboxylic acid **36**, and the amide **37** were an order of magnitude less potent. Compound **28** showed reduced potency in cells and whole blood. The tetrazole analogue **35** was the most potent analogue in the enzymatic assay; however, the ionization of the tetrazole ring most likely rendered this compound much less potent in cellular and blood assays (solubility⁴² of 0 $\mu\text{g}/\text{mL}$; PAMPA⁴² permeability of 0 at pH 7.4). Large substituents on the pyridyl ring of compounds **29**, **30**, and **32** were not favored, while smaller groups such as methyl (**31**) did not offer an advantage in potency. The one-carbon-atom homologated derivative **22** was 13-fold less active than **12**, and the imidazolylacetamide **23** was much less potent. Two triazole-containing analogues **51** and **55** had potencies comparable to those of compounds **11**, **12**, **28**, and **33** in the enzyme assay with improved potency in whole blood and were studied further (see below).

We further investigated the effect of substitution patterns on the imidazole tailpiece analogues and evaluated the resulting compounds in cellular and blood assays for the functional ability to inhibit the release of TNF- α with the goal of identifying several compounds for in vivo evaluation. A select group of these analogues, with either Cl or Br at the C-8 position, is shown in Table 3. In the enzymatic assay, N-1', C-5' analogues were the most potent followed C-2' substituted analogues. Substitution at the C-2' position alone reduced Tpl2 inhibition. For example, compounds **39–42**, **44**, **49**, and **50** were slightly to moderately more potent than compounds **45–48**. Although imidazole tailpiece analogues with substituted basic amino groups had improved solubility (36 $\mu\text{g}/\text{mL}$ for **43** and 69 $\mu\text{g}/\text{mL}$ for **49** compared to 2 $\mu\text{g}/\text{mL}$ for **12**), this property enhancement did not translate into increased potency in cells and blood. All compounds in Table 3 had IC₅₀ values of >5 μM against EGFR kinase autophosphorylation in A431 cells.

Selectivity. After identification of compounds with in vitro potency and selectivity for EGFR, seven compounds were chosen for further screening against a panel of kinases and for cytochrome P450 inhibition (3A4 isozyme). The panel included a number of serine–threonine kinases and kinases involved with TNF- α production (p38 α , MK2, IKK β , Jnk1) kinases with diverse biological functions and kinases that were deemed undesirable because of possible off-target toxicities (Table 4). Compounds **10**, **11**, **33**, **40**, **44**, **51**, and **55** demonstrated 200- to 1000-fold selectivity for Tpl2 in this panel and had moderate CYP3A4 inhibition.

Pharmacokinetics. Compounds **11**, **33**, **39**, **40**, **44**, **51**, and **55** were further evaluated for pharmacokinetic profiling in rats. Data for individual oral (po) and intravenous (iv) dosing parameters are shown in Table 5. Compounds **11** and **51** had moderate plasma clearance and moderate volumes of distribution, while compounds **33**, **40**, and **44** had high plasma clearance and moderate (**33**) or high (**40** and **44**) volumes of distribution. Compounds **11**, **33**, **51**, and **55** exhibited low oral bioavailability, possibly due to low aqueous solubility and/or permeability and/or a high first-pass effect. With the exception of **55**, all had solubilities of <10 $\mu\text{g}/\text{mL}$ and PAMPA⁴² permeability of <5.0 $\times 10^{-6}$ cm/s at pH 7.4. In contrast, compound **44** had higher oral bioavailability (42%). Compound **44** was advanced for an in vivo oral activity study in a rat model of TNF- α production.

In Vivo Study. Compound **44** was examined for the ability to inhibit the production of TNF- α in the LPS-induced rat model at an oral dose of 50 mg/kg. Compound **44** exhibited a statistically significant inhibition of TNF- α in female Sprague-Dawley rats (Figure 3). In this same study compound **3** showed an 85% inhibition of TNF- α , consistent with a previously determined ED₅₀ of 5 mg/kg in the corresponding mouse model.⁴ The average plasma concentration of compound **44** at 60 and 150 min postchallenge were 1.1 and 0.55 μM , respectively, which was closer to the cellular inhibition concentration of **44** (0.67 μM) than to the blood inhibition concentration (6.3 μM). Further biophysical and animal model studies will help to discern the pharmacodynamic relationship of potency in blood, plasma concentration, and in vivo efficacy.⁴³

Conclusions

Using X-ray crystallographic data and molecular modeling, we discovered a key structural addition that resulted in an improved selectivity profile for the cyanoquinoline series.

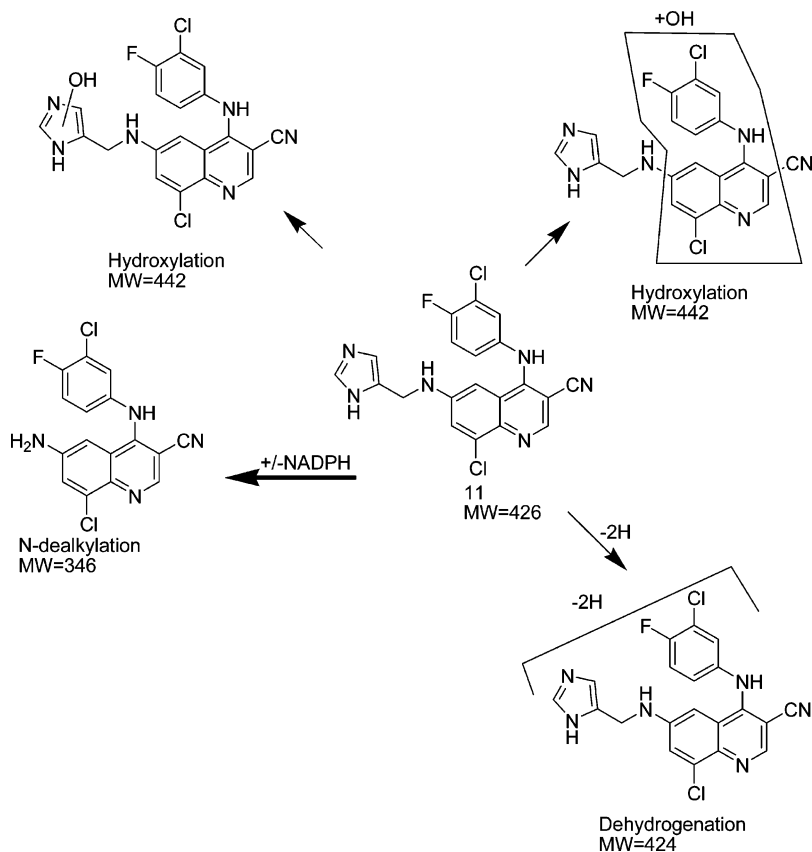


Figure 2. In vitro metabolic pathways of **11**.

Table 4. Selectivity Profiles of Compounds **10**, **11**, **33**, **40**, **44**, **51**, and **55**

kinase	IC ₅₀ (μM) ^a						
	10	11	33	40	44	51	55
p38α	>40	11.2	>40	>40	>40	3.6	>40
CAMKII	>40	>40	>40	>40	>40	>100	5.6
PKCα	>40	23.4	>40	>40	>40	>100	>40
PKA	10.3	40.1	>40	76.1	>100	>100	>40
MK2	>40	40.2	40.1	62.7	87.1	35.8	>40
Src	20	19.9	>40	>40	>40	40.8	>40
S6K	>40	>100	>40	18.8	83.1	>100	>40
Jnk1					31.0		>40
GSKβ					>10		
LYN					>30		
BTK					>10		
PKCθ					>50		
LCK					4.5		
CYP3A4	96% @ 3 μM	9.0	18.0	16.0	15.0	NT ^b	66% @ 3 μM

^a Average of at least two runs performed in duplicate with a standard deviation of 20%. ^b NT: not tested.

Introduction of functionality at the C-8 position resulted in reduced inhibition of other kinases including EGFR kinase. Further SAR investigations provided several quinoline-3-carbonitriles with improved potency in human blood (**11**, **33**, **40**, **44**, **51**, and **55**), one of which (**44**) had acceptable pharmacokinetic properties, including oral bioavailability. Compound **44** inhibited the LPS-induced production of TNF-α in the rat model. These results suggest that compounds in this series may have potential as therapeutic agents for the treatment of rheumatoid arthritis and other inflammatory diseases. The findings reported here provided insights into further lead optimization and in vivo studies, which will be reported in due course.

Table 5. Mean Pharmacokinetic Parameters of Compounds **11**, **33**, **40**, **44**, **51**, and **55** after iv or po Dosing in Female Sprague-Dawley Rats^a

parameters	11	33	40	44	51	55
iv Cl _p (mL min ⁻¹ kg ⁻¹)	19	38	>100	50	29	NT ^b
iv V _{ss} (L kg ⁻¹)	2.4	1.6	12.2	14.1	2.7	NT ^b
iv t _{1/2} (h)	4.4	0.8	1.2	5.0	3.2	NT ^b
po AUC _{0-inf} dose ⁻¹ (ng h kg mg ⁻¹ mL ⁻¹)	24	< 10	NT ^b	142	< 10	< 10
po C _{max}	61	< 10	NT ^b	511	34	< 10
po t _{1/2} (h)	8.1	4.2	NT ^b	4.0	3.9	2.6
F (%)	2	< 1	NT ^b	42	2	NT ^b

^a n = 3 animals per study. For iv: dosed 5 mg/kg in 50% DMSO, 50% PEG200 solution. For po: dosed 25 mg/kg in 2% Tween, 0.5% methylcellulose, 0.06% lactic acid in water. ^b NT: not tested.

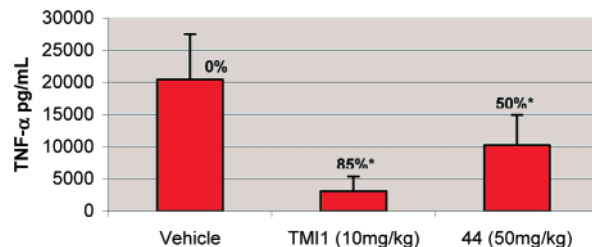


Figure 3. Compounds **44** and TMI-1 tested in LPS-induced TNF-α production in female Sprague-Dawley rats. Animals (average, 200 g) were pretreated (po) with **44** at 50 mg/kg and TMI-1 at 10 mg/kg. After 1 h the rats were challenged with LPS (iv, 1 mg/kg). Postchallenge (10 and 90 min) blood was drawn to determine compound plasma levels. TNF-α levels in plasma were measured by CBA: (*) *p* < 0.0015 by Student *T*-test.

Experimental Section

Chemistry. Reactions were run using commercially available starting materials and solvents without further purification. Proton NMR spectra were recorded at 400 MHz on a Bruker AV-400 spectrometer using TMS (δ 0.0) as a reference. Combustion

analyses were obtained using a Perkin-Elmer series II 2400 CHNS/O analyzer. CHN analyses were carried out by Robertson-Microlit. Where analyses are indicated by symbols of the elements, analytical results obtained for those elements were within ± 0.4 of the theoretical values. Low-resolution mass spectra were obtained using a Micromass Platform electrospray ionization quadrupole mass spectrometer. High-resolution mass spectra were obtained using a Bruker APEXIII Fourier transform ion cyclotron resonance (FT-ICR) mass spectrometer equipped with an actively shielded 7 T superconducting magnet (MagneX Scientific Ltd., U.K.) and an external Bruker APOLLO electrospray ionization (ESI) source. The microwave procedures were carried out with a Biotage microwave. Preparative HPLC was run using a Waters reverse-phase preparative HPLC with Xterra C18 5 μ M, 30 mm \times 100 mm column. The flow rate was 40 mL/min. Mobile phase A was water; mobile phase B was CH₃CN. Triethylamine was used as a modifier. Purity in the two solvent systems [H₂O–CH₃CN (HPLC method 1) and H₂O–MeOH (HPLC method 2)] was determined using an Agilent 1100 HPLC instrument.

The literature procedure for the synthesis of 4-anilinoquinoline-3-carbonitriles from nitroanilines (ref 21) was used to synthesize intermediates **8b–k** from substituted nitroanilines **4a–g**. See below for additional modifications and details.

8-Bromo-4-[(3-chloro-4-fluorophenyl)amino]-6-[(1*H*-imidazol-5-ylmethyl)amino]quinoline-3-carbonitrile (12). In a microwave vial, **7d** (4.00 g, 12.8 mmol) and 3-chloro-4-fluoroaniline (2.05 g, 14.1 mmol) were dissolved in 20 mL of EtOH. The vial was sealed and heated in a microwave reactor at 140 °C for 10 min. The cap was then removed, tin chloride dihydrate (16.00 g, 71 mmol) was added, and the vial was resealed and heated at 110 °C for 5 min. The contents of the vial were rinsed with EtOH into 300 mL of ice–water and neutralized with aqueous saturated NaHCO₃. The orange suspension was extracted with EtOAc (4 \times 300 mL). The combined organic layers were dried over anhydrous MgSO₄, filtered, and evaporated, and the crude product was purified by flash chromatography over silica gel (3–5% MeOH in CH₂Cl₂) to give **9d** (2.50 g, 50% yield) as a brown solid: ¹H NMR (400 MHz, DMSO-*d*₆) δ ppm 6.05 (s, 2 H), 7.29–7.34 (m, 2 H), 7.49–7.55 (m, 2 H), 7.77 (d, *J* = 2.3 Hz, 1 H), 8.53 (s, 1 H), 9.60 (s, 1 H); HRMS (ESI⁺) calcd for C₁₆H₁₀BrClFN₄ (MH⁺) 390.9756, found 390.9754. In a 1 L flask, **9d** (2.50 g, 6.38 mmol) and 4(5)-imidazolecarboxaldehyde (0.65 g, 6.38 mmol) were dissolved in 80 mL of THF and 35 mL of MeOH and stirred overnight. The solution was then acidified to pH 4 with HOAc, NaCNBH₃ (0.58 g, 9.3 mmol) was added, and the mixture was allowed to stir overnight again. Solvent was then removed under reduced pressure, and the crude product was purified by flash chromatography over silica gel (6–9% MeOH in CH₂Cl₂) and trituration with 165 mL of boiling EtOH to give **12** as a bright-yellow powder (1.35 g, 45% yield): ¹H NMR (400 MHz, DMSO-*d*₆) δ ppm 4.26 (d, *J* = 5.1 Hz, 2 H), 6.67 (t, *J* = 5.2 Hz, 1 H), 7.05 (s, 1 H), 7.25 (d, *J* = 2.3 Hz, 1 H), 7.26–7.32 (m, 1 H), 7.45 (t, *J* = 9.0 Hz, 1 H), 7.53 (dd, *J* = 6.6, 2.5 Hz, 1 H), 7.62 (s, 1 H), 7.79 (d, *J* = 2.0 Hz, 1 H), 8.38 (s, 1 H), 9.47 (s, 1 H), 11.96 (br s, 1 H); HRMS (ESI⁺) calcd for C₂₀H₁₄BrClFN₆ (MH⁺) 471.0131, found 471.0140. HPLC method 1: 98.6%, 4.15 min. HPLC method 2: 98.8%, 4.81 min.

By use of this same general procedure, all the compounds in this study were synthesized from intermediates **8b–k** unless otherwise noted.

4-[(3-Chloro-4-fluorophenyl)amino]-8-fluoro-6-[(1*H*-imidazol-5-ylmethyl)amino]quinoline-3-carbonitrile (10). Intermediate **7b** (0.60 g, 2.38 mmol) was dissolved with 3-chloro-4-fluoroaniline (0.42 g, 2.86 mmol) in 10 mL of EtOH and heated at 65 °C for 4 h. After workup, **8b** (0.7 g, 82% yield) was obtained as a yellow solid: ¹H NMR (400 MHz, DMSO-*d*₆) δ ppm 7.51–7.58 (m, 1 H), 7.62 (t, *J* = 8.97 Hz, 1 H), 7.82 (dd, *J* = 6.44, 2.15 Hz, 1 H), 8.59 (dd, *J* = 10.11, 2.02 Hz, 1 H), 8.91 (s, 1 H), 9.52 (s, 1 H), 10.73 (s, 1 H); HRMS (ESI⁺) calcd for C₁₆H₇ClF₂N₄O₂ (MH⁺) 361.029 83, found 361.0294. Reduction of **8b** (0.7 g, 2.15 mmol) with tin chloride dihydrate (2.4 g, 10.7 mmol) in 30 mL of EtOH afforded **9b** (710 mg, 100% yield) as a light-brown solid: ¹H NMR

(400 MHz, DMSO-*d*₆) δ ppm 5.94 (s, 2 H), 6.98–7.10 (m, 2 H), 7.15–7.29 (m, 1 H), 7.35–7.48 (m, 2 H), 8.26–8.39 (m, 1 H), 9.45 (br, s, 1 H); HRMS (ESI⁺) calcd for C₁₆H₉ClF₂N₄ (MH⁺) 331.05566, found 331.0562. The procedure described above for the synthesis of **12** was followed, reacting **9b** (70 mg, 0.21 mmol) with 4(5)-imidazolecarboxaldehyde (28 mg, 0.3 mmol) and NaCNBH₃ (9 mg, 0.1 mmol) in 2 mL of EtOH. The crude product was purified by preparative HPLC and lyophilized to give the product as a bright-yellow solid (26 mg, 31%): ¹H NMR (400 MHz, DMSO-*d*₆) δ ppm 4.19 (d, *J* = 5.05 Hz, 2 H), 6.61 (t, *J* = 5.05 Hz, 1 H), 6.95–7.07 (m, 2 H), 7.15 (d, *J* = 12.88, 2.02 Hz, 1 H), 7.19–7.28 (m, 1 H), 7.38 (t, *J* = 9.09 Hz, 1 H), 7.48 (dd, *J* = 6.57, 2.53 Hz, 1 H), 7.56 (d, *J* = 1.01 Hz, 1 H), 8.11 (s, 1 H), 8.23 (s, 1 H), 9.40 (s, 1 H); HRMS (ESI⁺) calcd for C₂₀H₁₃ClF₂N₆ (MH⁺) 411.093 10, found 411.0925. HPLC method 1: 95.9%, 3.88 min. HPLC method 2: 96.5%, 3.42 min.

8-Chloro-4-[(3-chloro-4-fluorophenyl)amino]-6-[(1*H*-imidazol-5-ylmethyl)amino]quinoline-3-carbonitrile (11). The procedure described above for the synthesis of **12** was followed, reacting **9c** (89 mg, 0.26 mmol) with 4(5)-imidazolecarboxaldehyde (28 mg, 0.29 mmol) and NaCNBH₃ (22 mg, 0.35 mmol) in 6 mL of EtOH. The crude product was purified by preparative HPLC and lyophilized to give **11** as a tan solid (65 mg, 60%): ¹H NMR (400 MHz, DMSO-*d*₆) δ ppm 4.26 (d, *J* = 5.05 Hz, 2 H), 6.67 (t, *J* = 5.43 Hz, 1 H), 7.05 (s, 1 H), 7.22 (d, *J* = 2.02 Hz, 1 H), 7.27–7.32 (m, 1 H), 7.45 (t, *J* = 8.97 Hz, 1 H), 7.53 (dd, *J* = 6.57, 2.78 Hz, 1 H), 7.57–7.63 (m, 2 H), 8.16 (s, 1 H), 8.38 (s, 1 H), 9.47 (s, 1 H); HRMS (ESI⁺) calcd for C₂₀H₁₃Cl₂FN₆ (MH⁺) 427.063 55, found 427.062. HPLC method 1: 99.3%, 4.01 min. HPLC method 2: 97.0%, 5.31 min. Anal. (C₂₀H₁₃Cl₂FN₆·HCO₂H) C, H, N: 53.29, 3.19, 17.76. Found: 52.84, 3.17, 17.59.

4-[(3-Chloro-4-fluorophenyl)amino]-6-[(1*H*-imidazol-5-ylmethyl)amino]-8-(trifluoromethyl)quinoline-3-carbonitrile (13). In a 100 mL round-bottomed flask equipped with a condenser, **7e** (2.44 g, 8.1 mmol) was dissolved in 35 mL of EtOH, and 3-chloro-4-fluoroaniline (1.41 g, 9.7 mmol) was added in one portion. The reaction mixture was heated at reflux for 1 h and then stirred at room temperature overnight. The EtOH was removed under reduced pressure, the residue was then partitioned between 50 mL of ether and 25 mL of aqueous saturated NaHCO₃ and stirred for 15 min. Partial concentration of the biphasic mixture gave a white solid that was filtered. The resulting solid was dried under vacuum overnight to give **8e** as a dark-yellow solid (3.3 g, 99%): ¹H NMR (400 MHz, DMSO-*d*₆) δ ppm 7.37–7.48 (m, 1 H), 7.53 (t, *J* = 8.97 Hz, 1 H), 7.71 (dd, *J* = 6.44, 2.40 Hz, 1 H), 8.79 (d, *J* = 2.27 Hz, 1 H), 8.87 (s, 1 H), 9.80 (d, *J* = 2.27 Hz, 1 H), 10.77 (s, 1 H); HRMS (ESI⁺) calcd for C₁₇H₇ClF₄N₄O₂ (MH⁺) 411.026 64, found 411.026. In a 100 mL round-bottomed flask equipped with a condenser, **8e** (1.65 g, 4.0 mmol) was dissolved in 50 mL of EtOH, and tin chloride dihydrate (4.53 g, 20.1 mmol) was added. The reaction mixture was heated at reflux for 1 h, then cooled to room temperature and poured into ice–water. The orange suspension was neutralized with aqueous saturated NaHCO₃ and extracted with CHCl₃ (3 \times 150 mL) and EtOAc (2 \times 150 mL). The combined organic layers were washed with brine, dried over anhydrous Na₂SO₄, filtered, and evaporated to give **9e** as a yellow solid (1.5 g, 98% yield): ¹H NMR (400 MHz, DMSO-*d*₆) δ ppm 3.92–4.12 (m, 1 H), 6.09 (s, 2 H), 7.15–7.31 (m, 1 H), 7.33–7.53 (m, 2 H), 7.70 (d, *J* = 2.27 Hz, 1 H), 8.44 (s, 1 H), 9.57 (s, 1 H); HRMS (ESI⁺) calcd for C₁₇H₂dClF₄N₄ (MH⁺) 381.052 46, found 381.053. The procedure described above for the synthesis of **12** was followed, reacting **9e** (150 mg, 0.39 mmol) with 4(5)-imidazolecarboxaldehyde (75 mg, 0.79 mmol) and NaCNBH₃ (37 mg, 0.72 mmol) in 5 mL of EtOH. The crude product was purified by preparative HPLC and lyophilized to give **13** as a yellow solid (137 mg, 76%): ¹H NMR (400 MHz, DMSO-*d*₆) δ ppm 4.31 (d, *J* = 5.31 Hz, 2 H), 6.82–6.91 (m, *J* = 5.31, 5.31 Hz, 1 H), 7.08 (s, 1 H), 7.28–7.37 (m, 1 H), 7.41–7.50 (m, 2 H), 7.57 (dd, *J* = 6.69, 2.65 Hz, 1 H), 7.66 (d, *J* = 1.01 Hz, 1 H), 7.86 (d, *J* = 2.27 Hz, 1 H), 8.41 (s, 1 H), 9.55 (s, 1 H), 12.18 (s, 1 H); HRMS (ESI⁺) calcd for

$C_{21}H_{13}ClF_4N_6$ (MH^+) 461.089 91, found 461.0903. HPLC method 1: 95.5%, 4.41 min. HPLC method 2: 95.7%, 5.34 min.

4-(3-Chloro-4-fluorophenylamino)-6-[(3*H*-imidazol-4-ylmethyl)amino]-8-methoxyquinoline-3-carbonitrile (15). The procedure for the synthesis of **12** was followed, reacting **9f** (190 mg, 0.55 mmol) with 4(5)-imidazolecarboxaldehyde (53 mg, 0.55 mmol) and $NaCNBH_3$ (24 mg, 0.39 mmol) in 8 mL of EtOH. The crude product was purified by preparative HPLC and lyophilized to give the product as a solid (33 mg, 14%): 1H NMR (400 MHz, DMSO- d_6) δ ppm 3.85 (s, 3 H), 4.22–4.27 (m, $J = 4.29$ Hz, 2 H), 6.34–6.41 (m, 1 H), 6.77 (d, $J = 1.77$ Hz, 1 H), 6.92 (s, 1 H), 7.05 (s, 1 H), 7.18–7.24 (m, 1 H), 7.38–7.45 (m, 2 H), 7.61 (d, $J = 1.01$ Hz, 1 H), 8.24 (s, 1 H), 9.21 (s, 1 H). HPLC method 1: 100.0%, 3.52 min. HPLC method 2: 100.0%, 2.85 min.

4-(3-Chloro-4-fluorophenylamino)-8-hydroxy-6-nitroquinoline-3-carbonitrile (8k). Intermediate **8f** (323 mg, 0.87 mmol), pyridine hydrochloride (130 mg, 1.12 mmol), and DMF (6 mL) were heated to 200 °C for 35 min in a microwave reactor. The crude product was purified by preparative HPLC and lyophilized to give **8k** as a solid (222 mg, 71%): 1H NMR (400 MHz, DMSO- d_6) δ ppm 7.43 (dd, $J = 6.82, 2.27$ Hz, 1 H), 7.51 (t, $J = 8.84$ Hz, 1 H), 7.69 (d, $J = 4.80$ Hz, 1 H), 7.83 (s, 1 H), 8.73 (s, 1 H), 8.98 (s, 1 H), 10.40 (s, 1 H), 10.89 (s, 1 H); HRMS (ESI^+) calcd for $C_{16}H_8ClFN_4O_3$ (MH^+) 359.034 17, found 359.034.

6-((1*H*-Imidazol-5-yl)methylamino)-4-(3-chloro-4-fluorophenylamino)-8-hydroxyquinoline-3-carbonitrile (14). The procedure for the synthesis of **12** was followed, reacting **8k** (176 mg, 0.49 mmol) with $SnCl_2 \cdot 2H_2O$ (547 mg, 2.42 mmol) in EtOH (5 mL) to give **9k** (160 mg, 99%): 1H NMR (400 MHz, DMSO- d_6) δ ppm 5.64 (s, 2 H), 6.59–6.67 (m, 2 H), 7.09–7.17 (m, 1 H), 7.32–7.43 (m, 2 H), 8.26 (s, 1 H), 9.24 (s, 1 H), 9.56 (s, 1 H); HRMS (ESI^+) calcd for $C_{16}H_{10}ClFN_4O$ (MH^+) 329.059 99, found 329.0601. Intermediate **9k** (122 mg, 0.37 mmol) was reacted with 4(5)-imidazolecarboxaldehyde (54 mg, 0.56 mmol) and $NaCNBH_3$ (30 mg, 0.48 mmol) in 10 mL of EtOH. The crude product was purified by preparative HPLC and lyophilized to give **14** as a tan solid (59 mg, 39%): 1H NMR (400 MHz, DMSO- d_6) δ ppm 4.16 (d, $J = 4.80$ Hz, 2 H), 6.25–6.33 (m, 1 H), 6.65–6.71 (m, 1 H), 6.94 (s, 1 H), 7.13–7.22 (m, 1 H), 7.33–7.42 (m, 2 H), 7.53 (d, $J = 1.26$ Hz, 1 H), 8.11 (s, 1 H), 8.18 (s, 1 H), 9.20 (s, 1 H), 9.42 (s, 1 H); HRMS (ESI^+) calcd for $C_{20}H_{14}ClFN_6O$ (MH^+) 409.097 44, found 409.0975. HPLC method 1: 91.4%, 3.53 min (broad). HPLC method 2: 100.0%, 2.96 min.

4-[(3-Chloro-4-fluorophenyl)amino]-6-[(1*H*-imidazol-5-ylmethyl)amino]-8-(methylsulfonyl)quinoline-3-carbonitrile (16). In a 50 mL round-bottomed flask, **6b** (0.50 g, 2.14 mmol) was dissolved in 9 mL of DMPU. $MeSNa$ (0.57 g, 8.1 mmol) was added, and the reaction mixture was stirred at room temperature overnight and poured into ice–water. An amount of 1 N HCl was added slowly until a copious precipitate formed. The mixture was filtered and the solid was washed with water to give a black solid. The crude product was purified by preparative HPLC to give **6h** as a yellow solid (0.21 g, 38%): 1H NMR (400 MHz, DMSO- d_6) δ ppm 2.72 (s, 3 H), 8.39 (d, $J = 2.27$ Hz, 1 H), 8.54–8.76 (m, 2 H), 12.45 (s, 1 H). In a 100 mL round-bottomed flask equipped with a condenser, **6h** (0.19 g, 0.71 mmol) was dissolved in 6 mL of $POCl_3$ and heated at reflux for 5 h. The reaction mixture was then stirred at room temperature overnight, and then $POCl_3$ was removed under reduced pressure. Ice chips were added to the residue, and then aqueous saturated $NaHCO_3$ solution was added carefully. The mixture was filtered and dried under high vacuum overnight to give **7h** as a brown solid (0.18 g, 90% yield): 1H NMR (400 MHz, DMSO- d_6) δ ppm 2.68 (s, 3 H), 8.21 (s, 1 H), 8.71 (s, 1 H), 9.40 (s, 1 H). The procedure described above for the synthesis of **12** was followed to convert **7h** to **8h**, isolated as a yellow solid (0.18 g, 72% yield): 1H NMR (400 MHz, DMSO- d_6) δ ppm 2.60 (s, 3 H), 7.41–7.48 (m, 1 H), 7.53 (t, $J = 8.97$ Hz, 1 H), 7.71 (dd, $J = 6.69, 2.40$ Hz, 1 H), 8.11 (d, $J = 2.02$ Hz, 1 H), 8.78 (s, 1 H), 9.26 (d, $J = 2.27$ Hz, 1 H), 10.52 (s, 1 H). To a solution of **8h** (50.0 mg, 0.13 mmol) in 2 mL of CH_2Cl_2 was added a solution of *m*-CPBA (28.8 mg, 0.13 mmol) in 2 mL of CH_2Cl_2 slowly

through an addition funnel at –5 °C. The reaction mixture was then stirred at –5 to 0 °C for 1.5 h, until TLC analysis showed complete disappearance of starting material. Aqueous saturated $NaHCO_3$ solution (5 mL) was added to the reaction mixture at 0 °C. The organic layer was washed with aqueous saturated $NaHCO_3$ solution and then washed with brine and concentrated to give **8i** as a yellow solid (56 mg, 100% yield): 1H NMR (400 MHz, DMSO- d_6) δ ppm 2.95 (s, 3 H), 7.38 (s, 1 H), 7.46–7.57 (m, 1 H), 7.65 (s, 1 H), 8.73 (d, $J = 2.27$ Hz, 2 H), 9.65 (d, $J = 3.03$ Hz, 1 H), 10.82 (s, 1 H). Reduction of **8i** using the procedure above for **12** gave **9i** as a dark-yellow solid (45 mg, 91% yield): 1H NMR (400 MHz, DMSO- d_6) δ ppm 2.42 (s, 3 H), 5.80 (s, 2 H), 6.88 (d, $J = 2.02$ Hz, 1 H), 7.01 (d, $J = 2.02$ Hz, 1 H), 7.13–7.16 (m, 1 H), 7.34–7.40 (m, 2 H), 8.33 (s, 1 H), 9.34 (s, 1 H). Reductive alkylation according to the procedure for **12**, reacting **9i** with 4(5)-imidazolecarboxaldehyde (21 mg, 0.22 mmol) and $NaCNBH_3$ (5 mg, 0.08 mmol) in 3 mL of EtOH, gave the product **16** as a tan solid (28 mg, 53%): 1H NMR (400 MHz, DMSO- d_6) δ ppm 2.39 (s, 3 H), 4.25 (d, $J = 5.05$ Hz, 2 H), 6.48 (d, 1 H), 6.95 (d, $J = 1.77$ Hz, 1 H), 7.05 (s, 1 H), 7.18 (d, $J = 2.02$ Hz, 1 H), 7.22–7.28 (m, 1 H), 7.38–7.51 (m, 2 H), 7.62 (d, $J = 1.01$ Hz, 1 H), 8.19 (s, 1 H), 8.30 (s, 1 H), 9.34 (s, 1 H); HRMS (ESI^+) calcd for $C_{21}H_{16}ClFN_6S$ (MH^+) 439.090 24, found 439.0898. HPLC method 1: 99.7%, 4.04 min. HPLC method 2: 98.5%, 4.69 min.

4-[(3-Chloro-4-fluorophenyl)amino]-6-[(1*H*-imidazol-5-ylmethyl)amino]-8-(methylsulfonyl)quinoline-3-carbonitrile (17). To a solution of **8h** (70 mg, 0.18 mmol) in 2 mL of THF was added a solution of *m*-CPBA (100 mg, 0.45 mmol) in 3 mL of THF slowly through an addition funnel at 0 °C. The reaction mixture was then stirred at 0 °C for 30 min, then at room temperature for 2 days. Aqueous saturated $NaHCO_3$ solution (5 mL) was added to the reaction mixture at 0 °C, and then 15 mL of EtOAc was added. The organic layer was washed with aqueous saturated $NaHCO_3$ solution and then washed with brine and concentrated to give **8j** as a light-brown solid (70 mg, 93% yield): 1H NMR (400 MHz, DMSO- d_6) δ ppm 3.47–3.61 (m, 3 H), 7.45–7.53 (m, 2 H), 7.56–7.67 (m, 2 H), 7.86–7.89 (m, 3 H). Reduction of **8j** using the procedure above for **12** gave **9j** isolated as a dark-yellow solid (50 mg, 77% yield). Reductive alkylation according to the procedure for **12**, reacting **9j** with 4(5)-imidazolecarboxaldehyde (20 mg, 0.22 mmol) and $NaCNBH_3$ (5 mg, 0.08 mmol) in 3 mL of EtOH, gave **17** as a yellow solid (9 mg, 15%): 1H NMR (400 MHz, DMSO- d_6) δ ppm 3.52 (s, 3 H), 4.32 (d, $J = 5.05$ Hz, 2 H), 7.04–7.08 (m, 1 H), 7.11 (t, $J = 5.81$ Hz, 1 H), 7.31–7.37 (m, 1 H), 7.47 (t, $J = 8.97$ Hz, 1 H), 7.51 (d, $J = 2.27$ Hz, 1 H), 7.58 (dd, $J = 6.57, 2.53$ Hz, 1 H), 7.61 (d, $J = 1.01$ Hz, 1 H), 8.12 (d, $J = 2.27$ Hz, 1 H), 8.28 (s, 1 H), 8.45 (s, 1 H); HRMS (ESI^+) calcd for $C_{21}H_{16}ClFN_6O_2S$ (MH^+) 471.080 07, found 471.0796. HPLC method 1: 95.0%, 4.02 min. HPLC method 2: 96.0%, 4.04 min.

4-[(3-Chloro-4-fluorophenyl)amino]-3-cyano-6-[(1*H*-imidazol-5-ylmethyl)amino]-*N,N*-dimethylquinoline-8-carboxamide (18). In a 2 L flask, 5-nitroanthranilic acid (100 g, 0.55 mol) and dimethylamine hydrochloride (50 g, 0.60 mol) were dissolved in 500 mL of DMF. Once both reagents had dissolved, benzotriazol-1-yloxytris(dimethylamino)phosphonium hexafluorophosphate (268 g, 0.604 mol) was added, followed by 4-methylmorpholine (134 mL, 1.21 mol). The mixture was stirred at room temperature overnight and then poured into 5 L of water and stirred vigorously until the suspension was evenly mixed. The precipitate was collected by suction filtration, washed with water, and dried under vacuum to give pure product 2-amino-*N,N*-dimethyl-5-nitrobenzamide **4g** as a yellow powder (103 g, 89% yield): 1H NMR (400 MHz, DMSO- d_6) δ ppm 2.93 (br s, 6 H), 6.69 (s, 2 H), 6.75 (d, $J = 9.4$ Hz, 1 H), 7.88 (d, $J = 2.8$ Hz, 1 H), 7.98 (dd, $J = 9.1, 2.8$ Hz, 1 H). In a 2 L flask, **4g** (103 g, 0.55 mol) and ethyl (ethoxymethylene)-cyanoacetate (188 g, 1.1 mol) were dissolved in 580 mL of DMF, and Cs_2CO_3 (362 g, 1.1 mol) was added. The mixture was heated to 45 °C for 2 h and then cooled to room temperature, stirred overnight, and poured into 5 L of water. The yellow precipitate was collected by suction filtration, washed generously three times with water, and dried under vacuum for 2 days to give pure ethyl

2-cyano-3-(2-(dimethylcarbamoyl)-4-nitrophenylamino)acrylate **5g** (174 g, 94% yield): $^1\text{H NMR}$ (400 MHz, DMSO- d_6) δ ppm 1.28 (t, $J = 7.1$ Hz, 3 H), 2.94 (s, 3 H), 3.06 (s, 3 H), 4.26 (q, $J = 7.2$ Hz, 2 H), 8.00 (d, $J = 9.4$ Hz, 1 H), 8.27 (d, $J = 2.5$ Hz, 1 H), 8.30–8.37 (m, 1 H), 8.72 (d, $J = 12.9$ Hz, 1 H), 11.34 (d, $J = 13.4$ Hz, 1 H). In a 2 L three-necked round-bottomed flask fitted with inert gas inlets/outlets and an internal device to monitor reaction temperature, **5g** (26.9 g, 80.9 mmol) was suspended in 1 L of Dowtherm A. Nitrogen gas was bubbled through each suspension for 40 min. The suspension was heated to 259 °C overnight, with inert gas gently flowing over the reaction mixture. After the mixture was allowed to cool to 50 °C, the contents were poured into 2.4 L of hexanes, stirred vigorously, and filtered, and the brown precipitate was washed twice with hexanes and once with EtOH and dried under vacuum overnight to give **6g** as a brown powder of sufficient purity to be used in the next step (28 g, 61% yield): $^1\text{H NMR}$ (400 MHz, DMSO- d_6) δ ppm 2.86 (s, 3 H), 3.09 (s, 3 H), 8.48 (d, $J = 2.5$ Hz, 1 H), 8.70 (s, 1 H), 8.85 (d, $J = 2.5$ Hz, 1 H), 12.61 (br s, 1 H). In a 1 L flask fitted with an addition funnel, **6g** (28 g, 98 mmol) was suspended in 200 mL of dichloroethane, and 1 mL of DMF was added. Oxalyl chloride (17 mL, 25 g, 0.20 mol) was then added dropwise via the addition funnel. After the addition was complete, the addition funnel was replaced with a reflux condenser, and the mixture was refluxed for 2 h. It was then allowed to cool to room temperature, and the solvent and excess oxalyl chloride were removed under reduced pressure. The residue was dissolved in CHCl_3 and passed over a short column of silica gel in a Büchner funnel, eluting with additional CHCl_3 . Evaporation of the solvent gave **7g** as a brown powder (13.8 g, 46% yield): $^1\text{H NMR}$ (400 MHz, DMSO- d_6) δ 2.69 (s, 3 H), 3.11 (s, 3 H), 8.64 (d, $J = 2.3$ Hz, 1 H), 9.06 (d, $J = 2.5$ Hz, 1 H), 9.43 (s, 1 H). The procedure described above for **12** gave **9g** (0.30 g, 0.78 mmol), which was reacted with 4(5)-imidazolecarboxaldehyde (75 mg, 0.78 mmol) and NaCNBH_3 (33 mg, 0.52 mmol). The crude product was purified by preparative HPLC and lyophilized to give **18** as a fluffy, bright-yellow solid (96 mg, 26% yield): $^1\text{H NMR}$ (400 MHz, DMSO- d_6) δ 2.67 (s, 3 H), 3.03 (s, 3 H), 4.28 (d, $J = 5.1$ Hz, 2 H), 6.62 (t, $J = 5.3$ Hz, 1 H), 7.05 (s, 1 H), 7.19–7.33 (m, 3 H), 7.44 (t, $J = 9.1$ Hz, 1 H), 7.53 (dd, $J = 6.6, 2.8$ Hz, 1 H), 7.62 (s, 1 H), 8.31 (s, 1 H), 9.47 (br s, 1 H); HRMS (ESI $^+$) calcd for $\text{C}_{23}\text{H}_{20}\text{ClFN}_7\text{O}$ (MH^+) 464.1397, found 464.1401. HPLC method 1: 98.6%, 3.86 min. HPLC method 2: 98.8%, 3.35 min. Anal. ($\text{C}_{23}\text{H}_{20}\text{ClFN}_7\text{O}$) C, H, N.

8-Acetyl-4-[(3-chloro-4-fluorophenyl)amino]-6-[(1H-imidazol-5-ylmethyl)amino]quinoline-3-carbonitrile (19). The iodide **9n** was prepared in a similar fashion to bromide **12** as shown in Scheme 1. To a microwave vial was added **9n** (50 mg, 0.10 mmol) tributyl-(1-ethoxyvinyl)stannane (52.2 mg, 0.14 mmol), and $\text{PdCl}_2(\text{PPh}_3)_2$ (6.8 mg, 0.01 mmol) in 2 mL of DMF. The vial was heated in a microwave reactor at 180 °C for 30 min. When the sample was cooled, 1 N HCl (1 mL) was added to the vial and the reaction mixture was stirred for 3 h at room temperature. The mixture was filtered through a pad of Celite and concentrated. The residue was purified via preparative HPLC to give the product as a yellow solid (5.8 mg, 14% overall yield): $^1\text{H NMR}$ (400 MHz, DMSO- d_6) δ ppm 2.69 (s, 3 H), 4.28 (d, $J = 5.05$ Hz, 2 H), 6.73 (t, 1 H), 7.04 (s, 1 H), 7.27–7.35 (m, 2 H), 7.38–7.48 (m, 2 H), 7.52–7.55 (m, 1 H), 7.61 (s, 1 H), 8.17 (s, 1 H), 8.36 (s, 1 H), 9.49 (s, 1 H), HRMS: calcd for $\text{C}_{22}\text{H}_{16}\text{ClFN}_6\text{O} + \text{H}^+$, 435.113 09; found (ESI-FTMS, $[\text{M} + \text{H}]^+$), 435.114. HPLC method 1: 98.0%, 4.55 min. HPLC method 2: 99.0%, 3.92 min.

4-[(3-Chloro-4-fluorophenyl)amino]-8-(2,3-dihydroxypropyl)-6-[(1H-imidazol-5-ylmethyl)amino]quinoline-3-carbonitrile (20). In a 20 mL microwave vial were added **9d** (500 mg, 1.3 mmol), DMF (15 mL), allyltributylstannane (630 mg, 1.9 mmol), and $\text{PdCl}_2(\text{PPh}_3)_2$ (100 mg, 0.13 mmol). The reaction mixture was heated in a microwave reactor at 180 °C for 30 min. The reaction mixture was diluted with water, and the aqueous layer was extracted three times with EtOAc. The combined EtOAc extracts were dried over MgSO_4 and concentrated. The residue was purified via preparative

HPLC and lyophilized to give **9m** as a yellow solid (214 mg, 48%). In a 15 mL round-bottom flask were added **9m** (214 mg, 0.6 mmol), dichloromethane (3 mL), pyridine (119 mg, 1.5 mmol), and trifluoroacetic anhydride (265 mg, 1.3 mmol) in that order. The mixture was stirred at room temperature for 4 h. The reaction mixture was diluted with water, and the aqueous layer was washed with EtOAc (3 \times). The combined EtOAc extracts were dried over MgSO_4 and concentrated. The crude acetamide (258 mg, 0.48 mmol) was dissolved in a 1:1 mixture of acetone and water (2 mL). To this were added OsO_4 (2.5 wt % in *t*-BuOH; 293 mg, 0.03 mmol) and NMO (112 mg, 0.96 mmol). The reaction mixture was stirred at room temperature for 4 h. To this was added 1 mL of 5 M LiOH solution, and the mixture was stirred for another 3 h. The heterogeneous mixture was filtered through a pad of Celite and washed with acetone and water. The filtrate was diluted with EtOAc, and the two layers were separated. The aqueous reaction mixture was extracted with EtOAc (2 \times). The combined EtOAc extracts were dried over MgSO_4 and concentrated to give crude **9n**. The residue (186 mg, 0.48 mmol) was dissolved in EtOH (2 mL), and 1H-imidazole-5-carbaldehyde (51 mg, 0.53 mmol) was added, followed by HOAc to bring the pH of the solution to 4. The mixture was stirred for 15 min. $\text{Na}(\text{OAc})_3\text{BH}$ (204 mg, 0.96 mmol) was then added, and the mixture was stirred at room temperature overnight. The reaction mixture was concentrated and the residue was purified via preparative HPLC and lyophilized to give **20** as a yellow solid (30 mg, 13%): $^1\text{H NMR}$ (400 MHz, MeOD) δ ppm 2.02–2.04 (m, 1 H), 2.66 (s, 1 H), 3.14 (dd, $J = 13.77, 7.71$ Hz, 1 H), 3.35 (s, 1 H), 3.52 (d, $J = 5.31$ Hz, 2 H), 3.94–4.02 (m, 1 H), 4.58 (s, 2 H), 7.13 (s, 1 H), 7.21–7.35 (m, 3 H), 7.38–7.47 (m, 2 H), 8.41 (s, 1 H), 8.81 (s, 1 H). HPLC method 1: 96.9%, 3.53 min. HPLC method 2: 97.7%, 3.01 min.

4-[(3-Chloro-4-fluorophenyl)amino]-8-(2,3-dihydroxypropoxy)-6-nitroquinoline-3-carbonitrile (8l). To a mixture of **8k** (274 mg, 0.77 mmol) and potassium carbonate (218 mg, 1.58 mmol) in DMF (7 mL) was added allyl bromide (0.073 mL, 0.84 mmol). After being stirred for 12 h at room temperature, the mixture was filtered, concentrated, and purified via preparative HPLC to give 4-[(3-chloro-4-fluorophenyl)amino]-8-allyloxy-6-nitroquinoline-3-carbonitrile as a tan solid (229 mg, 75%): $^1\text{H NMR}$ (400 MHz, DMSO- d_6) δ ppm 4.92 (d, $J = 5.31$ Hz, 2 H), 5.36 (dd, $J = 10.48, 1.64$ Hz, 1 H), 5.49–5.57 (m, 1 H), 6.11–6.23 (m, 1 H), 7.36 (s, 1 H), 7.49 (t, $J = 8.97$ Hz, 1 H), 7.62 (s, 1 H), 7.95 (d, $J = 2.27$ Hz, 1 H), 8.68 (s, 1 H), 9.08 (s, 1 H), 10.45 (s, 1 H). To a mixture of this intermediate in acetone (16 mL) and water (6 mL) was added 4-methylmorpholine *N*-oxide (235 mg, 2.01 mmol) followed by OsO_4 (0.5 mL, 2.5% in *t*-BuOH). After being stirred for 12 h at room temperature, the mixture was diluted with EtOAc, washed with water, dried over Na_2SO_4 , and concentrated. The crude product was purified via preparative HPLC to give **8l** as a tan solid (71 mg, 47%): $^1\text{H NMR}$ (400 MHz, DMSO- d_6) δ ppm 2.07 (s, 1 H), 4.33 (d, $J = 5.56$ Hz, 2 H), 5.03 (s, 2 H), 6.60 (s, 1 H), 6.83 (s, 1 H), 7.06 (s, 1 H), 7.19–7.26 (m, 2 H), 7.33–7.50 (m, 2 H), 7.70 (d, $J = 9.09$ Hz, 1 H), 8.33 (s, 1 H), 9.29 (s, 1 H); HRMS (ESI $^+$) calcd for $\text{C}_{19}\text{H}_{14}\text{ClFN}_4\text{O}_5$ (MH^+) 433.070 95, found 433.0705. HPLC method 1: 97.1%, 4.54 min. HPLC method 2: 99.6%, 5.69 min.

4-[(3-Chloro-4-fluorophenyl)amino]-8-(2,3-dihydroxypropoxy)-6-[(1H-imidazol-5-ylmethyl)amino]quinoline-3-carbonitrile (21). Reduction and reductive alkylation of **8l** using the method for the synthesis of **12** gave **21** as an orange solid (10 mg, 25%): $^1\text{H NMR}$ (400 MHz, DMSO- d_6) δ ppm 2.65–2.69 (m, 1 H), 3.49–3.55 (m, 2 H), 3.98 (dd, $J = 9.09, 6.32$ Hz, 2 H), 4.08–4.13 (m, 1 H), 4.22–4.27 (m, 2 H), 4.72–4.77 (m, 1 H), 6.32–6.42 (m, 1 H), 6.82 (s, 1 H), 6.97 (s, 1 H), 7.03 (s, 1 H), 7.22 (d, $J = 9.09$ Hz, 1 H), 7.41 (d, $J = 9.09$ Hz, 2 H), 7.61 (s, 1 H), 8.25–8.34 (m, 2 H), 9.25 (s, 1 H); HRMS (ESI $^+$) calcd for $\text{C}_{23}\text{H}_{20}\text{ClFN}_6\text{O}_3$ (MH^+) 483.134 22, found 483.1328. HPLC method 1: 98.9%, 3.24 min. HPLC method 2: 98.3%, 2.25 min.

8-Chloro-4-[(3-chloro-4-fluorophenyl)amino]-6-[[2-(1H-imidazol-5-yl)ethyl]amino]quinoline-3-carbonitrile (22). In a mi-

crowave vial, methoxymethyltriphenylphosphonium bromide (300 mg, 0.77 mmol) was dissolved in 4 mL of THF, and NaH (46 mg, 0.46 mmol) was added. The vial was sealed and heated in a microwave reactor at 80 °C for 5 min. Then tritylimidazolealdehyde (104 mg, 0.31 mmol) was added and the reaction mixture was stirred at room temperature for 3 h. The solvent was removed and the crude product was purified by flash chromatography over silica gel (5% MeOH in CH₂Cl₂) to give 5-(2-methoxyvinyl)-1-trityl-1*H*-imidazole as a white solid (90 mg, 79% yield). In a 50 mL round-bottomed flask equipped with a condenser, 5-(2-methoxyvinyl)-1-trityl-1*H*-imidazole (90 mg, 0.25 mmol) was dissolved in 5 mL of 1 N HCl and 3 mL of THF and heated at 60 °C for 2 h. The reaction mixture was then allowed to cool to room temperature, and the solvent was removed to give (3*H*-imidazol-4-yl)acetaldehyde as a white solid of sufficient purity to be used in the next step (26 mg, 96% yield). The procedure described above for the synthesis of **12** was followed reacting **9c** (85 mg, 0.24 mmol) with (3*H*-imidazol-4-yl)acetaldehyde (26 mg, 0.24 mmol) and NaCNBH₃ (13 mg, 0.22 mmol) in 5 mL of EtOH. The crude product was purified by preparative HPLC and lyophilized to give a yellow solid (15 mg, 14%): ¹H NMR (400 MHz, DMSO-*d*₆) δ ppm 2.83 (t, *J* = 7.07 Hz, 2 H), 3.31–3.44 (m, 2 H), 6.56 (t, *J* = 5.68 Hz, 1 H), 6.87 (s, 1 H), 7.12 (d, *J* = 2.27 Hz, 1 H), 7.24–7.35 (m, 1 H), 7.45 (t, *J* = 9.09 Hz, 1 H), 7.49 (d, *J* = 2.27 Hz, 1 H), 7.51–7.60 (m, 2 H), 8.20 (s, 1 H), 8.37 (s, 1 H), 9.53 (s, 1 H); HRMS (ESI⁻) calcd for C₂₁H₁₅Cl₂FN₆ (MH⁻) 439.064 65, found 439.0661. HPLC method 1: 99.0%, 4.11 min. HPLC method 2: 99.0%, 4.55 min.

N-(8-Bromo-4-(3-chloro-4-fluorophenylamino)-3-cyanoquinolin-6-yl)-2-(1*H*-imidazol-5-yl)acetamide (23). A solution of **9d** (500 mg, 1.28 mmol), imidazoleacetic acid hydrochloride (228 mg, 1.40 mmol), benzotriazol-1-yloxytris(dimethylamino)phosphonium hexafluorophosphate (619 mg, 1.40 mmol), and 4-methylmorpholine (0.31 mL, 0.29 g, 2.8 mmol) in 10 mL pf DMF was heated at 60 °C overnight. Additional imidazoleacetic acid hydrochloride (847 mg), benzotriazol-1-yloxytris(dimethylamino)phosphonium hexafluorophosphate (2.48 g), and 4-methylmorpholine (2.1 mL) were added, and stirring continued at room temperature for 3 days. The reaction mixture was poured into 100 mL of water, and the dark-brown precipitate was collected by suction filtration, washed with water, and dried under vacuum. This crude product was then purified twice by preparative HPLC and lyophilized to give **23** as a pale-yellow powder (76 mg, 12% yield): ¹H NMR (400 MHz, DMSO-*d*₆) δ ppm 3.64 (s, 2 H), 6.98 (s, 1 H), 7.28 (ddd, *J* = 8.8, 4.2, 2.9 Hz, 1 H), 7.44 (t, *J* = 9.0 Hz, 1 H), 7.52 (dd, *J* = 6.6, 2.8 Hz, 1 H), 7.60 (s, 1 H), 8.38 (d, *J* = 2.0 Hz, 1 H), 8.61–8.70 (m, 2 H), 9.95 (s, 1 H), 10.54 (s, 1 H), 12.21 (s, 1 H); HRMS (ESI⁺) calcd for C₂₁H₁₄BrClFN₆O (MH⁺) 499.0080, found 499.0071. HPLC method 1: 99.0%, 4.12 min. HPLC method 2: 99.0%, 4.80 min.

8-Chloro-4-[(3-chloro-4-fluorophenyl)amino]-6-[(1-methyl-1*H*-pyrazol-4-yl)methylamino]quinoline-3-carbonitrile (24). In a test tube were added **9c** (50 mg), dichloroethane (2 mL), and 1-methyl-1*H*-pyrazole-4-carbaldehyde (1.2 equiv). The mixture was stirred for 15 min at room temperature. Na(OAc)₃BH (2 equiv) was then added, and the mixture was stirred at room temperature for 6 h. The reaction mixture was concentrated and the residue was purified to give **24** (29 mg): ¹H NMR (400 MHz, MeOD) δ ppm 4.44–4.53 (m, 2 H), 7.31 (s, 1 H), 7.40–7.54 (m, 2 H), 7.59–7.65 (m, 1 H), 7.69 (s, 1 H), 7.79 (s, 1 H), 8.53 (s, 1 H), 8.77 (s, 1 H). HPLC method 1: 100.0%, 5.24 min. HPLC method 2: 99.6%, 6.46 min.

8-Bromo-4-(3-chloro-4-fluorophenylamino)-6-[(2-methyl-2*H*-pyrazol-3-ylmethylamino]quinoline-3-carbonitrile (25). The procedure described above for the synthesis of **12** was followed, reacting **9c** (80 mg, 0.20 mmol), 2-methyl-2*H*-pyrazole-3-carbaldehyde (20 mg, 0.24 mmol), and NaCNBH₃ (17 mg, 0.27 mmol) in 3 mL of EtOH and 5 drops of HOAc. Concentration of the mixture gave a brown semisolid, which was dissolved in 2 mL of DMSO. Purification by HPLC afforded **25** (5 mg, 5%) as a yellow solid. ¹H NMR (400 MHz, DMSO-*d*₆) δ ppm 3.81 (s, 3 H), 4.42

(d, *J* = 5.56 Hz, 2 H), 6.26 (d, *J* = 2.02 Hz, 1 H), 6.87 (t, *J* = 5.56 Hz, 1 H), 7.21–7.31 (m, 3 H), 7.32 (d, *J* = 2.02 Hz, 1 H), 7.39–7.49 (m, 1 H), 7.48–7.55 (m, 1 H), 7.75 (s, 1 H), 8.40 (s, 1 H), 8.43 (s, 1 H); HRMS (ESI⁺) calcd for C₂₁H₁₅BrClFN₆ (MH⁺) 485.028 69, found (ESI-FTMS, [M + H]⁺), 485.0277. HPLC method 1: 99.0%, 5.45 min. HPLC method 2: 99.0%, 6.70 min.

8-Bromo-4-(3-chloro-4-fluorophenylamino)-6-[(2-phenyl-2*H*-pyrazol-3-ylmethylamino]quinoline-3-carbonitrile (26). The procedure described above for the synthesis of **12** was followed, reacting **9c** (80 mg, 0.20 mmol), 1-phenyl-2*H*-pyrazole-5-carbaldehyde (49 mg, 0.28 mmol), and NaCNBH₃ (17 mg, 0.27 mmol) in 3 mL of EtOH and 5 drops of HOAc. Concentration of the mixture gave a brown semisolid, which was dissolved in 2 mL of DMSO. Purification by HPLC afforded **26** (16 mg, 11%) as a yellow solid. ¹H NMR (400 MHz, DMSO-*d*₆) δ ppm 4.48 (s, 2 H), 6.59 (d, *J* = 1.77 Hz, 1 H), 7.24 (d, *J* = 1.77 Hz, 1 H), 7.27–7.37 (m, 1 H), 7.44–7.52 (m, 2 H), 7.52–7.60 (m, 4 H), 7.61–7.67 (m, 2 H), 7.73 (d, *J* = 1.77 Hz, 1 H), 7.81 (d, *J* = 2.27 Hz, 1 H), 8.48 (s, 1 H), 9.46 (s, 1 H); HRMS (ESI⁺) calcd for C₂₆H₁₇BrClFN₆ (MH⁺) 547.044 34, found (ESI-FTMS, [M + H]⁺), 547.0437. HPLC method 1: 97.0%, 6.12 min. HPLC method 2: 97.0%, 7.18 min.

8-Bromo-4-[(3-chloro-4-fluorophenyl)amino]-6-[(imidazo[1,2-*a*]pyridin-3-ylmethylamino]quinoline-3-carbonitrile (27). The procedure described above for the synthesis of **12** was followed, reacting **9c** (40 mg, 0.10 mmol) with 1*H*-imidazo[1,2-*a*]pyridine-3-carbaldehyde, (18 mg, 0.12 mmol) and NaCNBH₃ (7 mg, 0.12 mmol) in 10 mL of EtOH. The reaction mixture was concentrated and the residue was purified via preparative HPLC and lyophilized to give **27** as a yellow solid (35 mg, 65%): ¹H NMR (400 MHz, DMSO-*d*₆) δ ppm 4.73 (d, *J* = 5.05 Hz, 2 H), 6.53 (s, 1 H), 6.93–7.01 (m, 2 H), 7.25–7.34 (m, 2 H), 7.46 (t, *J* = 9.09 Hz, 1 H), 7.55 (dd, *J* = 6.57, 2.78 Hz, 1 H), 7.60 (d, *J* = 9.09 Hz, 1 H), 7.68 (s, 1 H), 7.71 (d, *J* = 2.27 Hz, 1 H), 8.39 (d, *J* = 6.82 Hz, 1 H), 8.41 (s, 1 H), 9.52 (s, 1 H); HRMS (ESI⁺) calcd for C₂₄H₁₅BrClFN₆ (MH⁺) 521.028 69, found 521.0302. HPLC method 1: 95.5%, 4.38 min. HPLC method 2: 95.8%, 5.25 min.

8-Chloro-4-(3-chloro-4-fluorophenylamino)-6-(pyridin-3-ylmethylamino)quinoline-3-carbonitrile (28). The procedure described above for the synthesis of **12** was followed, reacting **9c** (87 mg, 0.25 mmol) with nicotinaldehyde (0.02 mL, 0.28 mmol) and NaCNBH₃ (22 mg, 0.35 mmol) in 9 mL of EtOH. The crude product was purified by preparative HPLC and lyophilized to give **28** as a tan solid (52 mg, 47%): ¹H NMR (400 MHz, DMSO-*d*₆) δ ppm 4.44 (d, *J* = 5.81 Hz, 2 H), 6.51 (d, 1 H), 7.01 (t, *J* = 5.94 Hz, 1 H), 7.21 (d, *J* = 2.27 Hz, 1 H), 7.24–7.29 (m, 1 H), 7.37 (dd, *J* = 8.21, 5.18 Hz, 1 H), 7.43 (t, *J* = 9.09 Hz, 1 H), 7.51 (dd, *J* = 6.57, 2.78 Hz, 1 H), 7.55 (d, *J* = 2.27 Hz, 1 H), 7.77–7.80 (m, 1 H), 8.13 (s, 1 H), 8.40 (s, 1 H), 8.48 (dd, *J* = 4.67, 1.64 Hz, 1 H), 8.62 (d, *J* = 1.77 Hz, 1 H), 9.44 (s, 1 H); HRMS (ESI⁺) calcd for C₂₂H₁₄Cl₂FN₅ (MH⁺) 438.068 30, found 438.0675. HPLC method 1: 99.1%, 4.41 min. HPLC method 2: 99.0%, 5.51 min.

8-Chloro-4-[(3-chloro-4-fluorophenyl)amino]-6-[(5-[2,2,2-trifluoro-1-hydroxy-1-(trifluoromethyl)ethyl]pyridin-3-yl)methylamino]quinoline-3-carbonitrile (29). To a mixture of 3,5-dibromopyridine (1.09 g, 4.60 mmol) in dry THF (20 mL) under a nitrogen atmosphere was added isopropylmagnesium chloride (2.4 mL, 2.0 M in THF, 4.8 mmol) dropwise. After 2 h, 1,1,1,3,3,3-hexafluoropropan-2-one was introduced into the reaction mixture slowly. After another hour, water (2 mL) was added to the reaction mixture. The mixture was diluted with CHCl₃ (500 mL), washed with H₂O (200 mL), and dried over MgSO₄, and the organic layer was concentrated. Purification (SiO₂, 8–25% EtOAc/hexane) gave 2-(5-bromopyridin-3-yl)-1,1,1,3,3,3-hexafluoropropan-2-ol (1.06 g, 71%) as a thick oil. To a mixture of 2-(5-bromopyridin-3-yl)-1,1,1,3,3,3-hexafluoropropan-2-ol (347 mg, 1.07 mmol) in dry THF (15 mL) under a nitrogen atmosphere was added isopropylmagnesium chloride (1.2 mL, 2.0 M in THF, 2.4 mmol) dropwise. After 1 h, DMF (150 μL, 1.94 mmol) was added. After another 2 h, HOAc

(400 μL) was added. The solvent was removed to give crude 5-(1,1,1,3,3,3-hexafluoro-2-hydroxypropan-2-yl)nicotinaldehyde, which was used in the next step without further purification. The procedure described above for the synthesis of **12** was followed, reacting **9c** (78 mg, 0.23 mmol) with this crude aldehyde, HOAc (100 μL), and NaCNBH₃ (25 mg, 0.40 mmol) in 1 mL of EtOH and 6 mL of DMF. After 12 h, the solvent was removed to minimum volume and the mixture was filtered. Purification using preparative HPLC gave **29** as a yellow solid (31 mg, 22%). ¹H NMR (400 MHz, DMSO-*d*₆) δ ppm 4.55 (d, *J* = 6.06 Hz, 2H), 7.13 (t, *J* = 5.94 Hz, 1H), 7.21–7.28 (m, 2H), 7.40–7.50 (m, 2H), 7.54 (d, *J* = 2.27 Hz, 1H), 8.09 (s, 1H), 8.39 (s, 1H), 8.74 (d, *J* = 2.02 Hz, 1H), 8.78 (d, *J* = 2.02 Hz, 1H), 9.06 (s, 1H), 9.42 (s, 1H); HRMS calcd for C₂₅H₁₄Cl₂F₇N₅O + H⁺, 604.053 64, found (ESI-FTMS, [M + H]⁺), 604.0533. HPLC method 1: 97.7%, 5.80 min. HPLC method 2: 100.0%, 6.97 min.

8-Chloro-4-[(3-chloro-4-fluorophenyl)amino]-6-[[5-(4-hydroxy-1-isopropylpiperidin-4-yl)pyridin-3-yl]methyl]amino}quinoline-3-carbonitrile (30). To a mixture of 3,5-dibromopyridine (1.4 g, 6.16 mmol) in dry THF (12 mL) under a nitrogen atmosphere was added isopropylmagnesium chloride (3.7 mL, 2.0 M in THF, 7.4 mmol) dropwise. After 2 h, *tert*-butyl 4-oxopiperidine-1-carboxylate (1.35 g, 6.78 mmol) in THF (6 mL) was slowly added. After 12 h, the mixture was diluted with EtOAc (500 mL), washed with H₂O (200 mL), and dried over MgSO₄. The organic layer was concentrated. Purification (SiO₂, 1–8% MeOH/CH₂Cl₂) gave *tert*-butyl 4-(5-bromopyridin-3-yl)-4-hydroxypiperidine-1-carboxylate (415 mg, 19%). To a mixture of *tert*-butyl 4-(5-bromopyridin-3-yl)-4-hydroxypiperidine-1-carboxylate (415 mg, 1.17 mmol) in dry THF (12 mL) under a nitrogen atmosphere was added isopropylmagnesium chloride (1.3 mL, 2.0 M in THF, 2.6 mmol) dropwise. After 12 h, DMF (0.25 mL, 3.23 mmol) was added. After another 2 h, HOAc (400 μL) was added. The solvent was removed to give crude *tert*-butyl 4-(5-formylpyridin-3-yl)-4-hydroxypiperidine-1-carboxylate, which was used in the next step without further purification. The procedure described above for the synthesis of **12** was followed, reacting **9c** (204 mg, 0.56 mmol) with the above aldehyde, HOAc (150 μL), and NaCNBH₃ (50 mg, 0.80 mmol) in 6 mL of DMF. After 12 h, purification using preparative HPLC gave the BOC-protected precursor as a yellow solid (177 mg, 50%). MS (*m/z*): M⁺, 637.2; M⁻, 635.6. To a mixture of this product (125 mg) in CH₂Cl₂ (3 mL) was added TFA (3 mL). After 1 h, the solvent was removed. Purification using HPLC gave the deprotected amine in quantitative yield. MS (*m/z*): M⁺, 537.1; M⁻, 535.5. To this amine (31 mg, 0.06 mmol) in acetone (4 mL) was added Na(OAc)₃BH (30 mg, 0.14 mmol). After 2 h, purification using preparative HPLC gave **30** as an off-white solid (5 mg). ¹H NMR (400 MHz, DMSO-*d*₆) δ ppm 1.00 (d, *J* = 6.57 Hz, 6H), 1.57 (d, *J* = 12.13 Hz, 2H), 1.83–1.95 (m, 2H), 2.53–2.62 (m, 4H), 2.70–2.80 (m, 1H), 4.44 (d, *J* = 5.81 Hz, 2H), 5.00 (s, 1H), 7.11 (t, *J* = 6.19 Hz, 1H), 7.20 (d, *J* = 2.02 Hz, 1H), 7.24–7.31 (m, 1H), 7.45 (t, *J* = 9.09 Hz, 1H), 7.50–7.55 (m, 2H), 7.95 (t, *J* = 2.15 Hz, 1H), 8.38 (s, 1H), 8.48 (d, *J* = 2.02 Hz, 1H), 8.57 (t, *J* = 2.15 Hz, 1H), 9.47 (s, 1H). MS (*m/z*) M⁺, 565.1; M⁻, 563.6. HPLC method 1: 99.5%, 3.98 min. HPLC method 2: 98.4%, 3.74 min.

8-Chloro-4-[(3-chloro-4-fluorophenyl)amino]-6-[[6-methylpyridin-2-yl]methyl]amino}quinoline-3-carbonitrile (31). The procedure described above for the synthesis of **12** was followed, reacting **9c** (80 mg, 0.23 mmol) with 6-methylpicolinaldehyde (120 mg, 0.99 mmol) and NaCNBH₃ (24 mg, 0.38 mmol) in 6 mL of EtOH. The crude product was purified by preparative HPLC and lyophilized to give **31** as a light-yellow solid (62 mg, 59%): ¹H NMR (400 MHz, DMSO-*d*₆) δ ppm 2.46 (s, 3H), 4.49 (d, *J* = 6.06 Hz, 2H), 7.06 (t, *J* = 5.94 Hz, 1H), 7.14 (dd, *J* = 9.85, 7.83 Hz, 2H), 7.19 (d, *J* = 2.27 Hz, 1H), 7.21–7.26 (m, 1H), 7.41 (t, *J* = 8.97 Hz, 1H), 7.47 (dd, *J* = 6.57, 2.53 Hz, 1H), 7.60–7.67 (m, 2H), 8.39 (s, 1H), 9.45 (s, 1H); HRMS (ESI⁺) calcd for C₂₃H₁₆Cl₂FN₅ (MH⁺) 452.083 95, found 452.0834. HPLC method 1: 99.0%, 4.72 min. HPLC method 2: 99.2%, 6.17 min.

8-Chloro-4-[(3-chloro-4-fluorophenyl)amino]-6-[[6-morpholin-4-ylpyridin-2-yl]methyl]amino}quinoline-3-carbonitrile (32). The procedure described above for the synthesis of **12** was followed, reacting **9c** (80 mg, 0.23 mmol) with 6-morpholin-4-ylpyridine-2-carbaldehyde (49 mg, 0.25 mmol) and NaCNBH₃ (10 mg, 0.16 mmol) in 4 mL of EtOH. The crude product was purified by preparative HPLC and lyophilized to give **32** as a yellow solid (55 mg, 46%): ¹H NMR (400 MHz, DMSO-*d*₆) δ ppm 3.37–3.51 (m, 4H), 3.61–3.73 (m, 4H), 4.36 (d, *J* = 6.06 Hz, 2H), 6.68 (t, *J* = 7.83 Hz, 2H), 6.92 (t, *J* = 6.06 Hz, 1H), 7.17–7.31 (m, 2H), 7.42 (t, *J* = 8.97, 1H), 7.45–7.55 (m, 2H), 7.65 (d, *J* = 2.27 Hz, 1H), 8.39 (s, 1H), 9.46 (s, 1H); HRMS (ESI⁺) calcd for C₂₂H₂₁Cl₂FN₆O (MH⁺) 523.121 07, found 523.1207. HPLC method 1: 96.3%, 5.78 min. HPLC method 2: 96.5%, 7.07 min.

8-Chloro-4-[(3-chloro-4-fluorophenyl)amino]-6-[[1-oxidopyridin-2-yl]methyl]amino}quinoline-3-carbonitrile (33). The procedure described above for the synthesis of **12** was followed, reacting **9c** (97 mg, 0.28 mmol) with pyridine-2-carbaldehyde-1-oxide (71 mg, 0.58 mmol) and NaCNBH₃ (35 mg, 0.56 mmol) in 10 mL of EtOH. The crude product was purified by preparative HPLC to **33** as a yellow solid (64 mg, 50%): ¹H NMR (400 MHz, DMSO-*d*₆) δ ppm 4.52 (d, *J* = 6.06 Hz, 2H), 6.98 (t, *J* = 5.94 Hz, 1H), 7.08 (d, *J* = 2.02 Hz, 1H), 7.14–7.37 (m, 5H), 7.42 (d, *J* = 5.56 Hz, 1H), 7.55 (s, 1H), 8.24–8.27 (m, 1H), 8.30 (s, 1H), 9.41 (s, 1H); HRMS (ESI⁺) calcd for C₂₂H₁₄Cl₂FN₅O (MH⁺) 454.063 22, found 454.0628. HPLC method 1: 100.0%, 4.82 min. HPLC method 2: 95.8%, 6.21 min.

8-Chloro-4-[(3-chloro-4-fluorophenyl)amino]-6-[(2,3-dihydroxypropyl)amino]quinoline-3-carbonitrile (34). The procedure described above for the synthesis of **12** was followed, reacting **9c** (148 mg, 0.43 mmol) with 2,3-dihydroxypropanal (55 mg, 0.61 mmol), HOAc (150 μL), and NaCNBH₃ (40 mg, 0.64 mmol) in 10 mL of EtOH. After 12 h, the reaction mixture was concentrated. Purification using HPLC gave **29** as a yellow solid (140 mg, 77%). ¹H NMR (400 MHz, DMSO-*d*₆) δ ppm 3.04–3.12 (m, 1H), 3.23–3.31 (m, 1H), 3.40–3.46 (m, 2H), 3.68–3.77 (m, 1H), 4.67 (t, *J* = 5.43 Hz, 1H), 4.90 (d, *J* = 5.05 Hz, 1H), 6.36 (t, *J* = 5.31 Hz, 1H), 7.08 (d, *J* = 2.27 Hz, 1H), 7.26–7.31 (m, 1H), 7.45 (t, *J* = 8.97 Hz, 1H), 7.52 (dd, *J* = 6.57, 2.78 Hz, 1H), 7.61 (d, *J* = 2.53 Hz, 1H), 8.36 (s, 1H), 9.48 (s, 1H). HPLC method 1: 97.1%, 4.54 min. HPLC method 2: 99.6%, 5.69 min.

8-Chloro-4-[(3-chloro-4-fluorophenyl)amino]-6-[(1*H*-tetrazol-5-ylmethyl)amino]quinoline-3-carbonitrile (35). In a 100 mL round-bottomed flask, diethoxy acetonitrile (1.0 g, 7.7 mmol) was dissolved in 35 mL of dichloroethane. Azidotributyltin (3.34 g, 10.1 mmol) was added, and the reaction mixture was heated at reflux temperature overnight. The reaction mixture was then concentrated to a black residue, dissolved in 20 mL of 1.25 M HCl in MeOH, and heated at 65 °C for 3 h, then allowed to cool to room temperature. Evaporation of the solvent gave 1*H*-tetrazole-5-carbaldehyde as a black oil, which was used directly in the next step without purification. The procedure described above for the synthesis of **12** was followed, reacting **9c** (200 mg, 0.58 mmol) with 1*H*-tetrazole-5-carbaldehyde (141.2 mg, 1.44 mmol) and NaCNBH₃ (25.3 mg, 0.40 mmol) in 5 mL of EtOH. The crude product was purified by preparative HPLC and lyophilized to give **35** as a yellow solid (17 mg, 7%): ¹H NMR (400 MHz, DMSO-*d*₆) δ ppm 4.45 (d, *J* = 5.05 Hz, 2H), 6.74 (t, *J* = 4.93 Hz, 1H), 7.26 (d, *J* = 2.27 Hz, 1H), 7.28–7.34 (m, 1H), 7.45 (t, *J* = 9.09 Hz, 1H), 7.54 (dd, *J* = 6.57, 2.78 Hz, 1H), 7.68 (d, *J* = 2.27 Hz, 1H), 8.37 (s, 1H), 9.54 (s, 1H); HRMS (ESI⁺) calcd for C₁₈H₁₁Cl₂FN₈ (MH⁺) 429.054 05, found 429.0539. HPLC method 1: 99.2%, 4.75 min. HPLC method 2: 99.8%, 4.90 min.

2-(8-Chloro-4-(3-chloro-4-fluorophenylamino)-3-cyanoquinolin-6-ylamino) Acetic Acid (36). The procedure described above for the synthesis of **12** was followed, reacting **9c** (301 mg, 0.77 mmol) with 2-oxoacetic acid (100 mg, 1.09 mmol), HOAc (150 μL), and NaCNBH₃ (50 mg, 0.80 mmol) in 10 mL of EtOH. Purification using HPLC gave **36** as a yellow solid (140 mg, 41%). ¹H NMR (400 MHz, DMSO-*d*₆) δ ppm 3.98 (d, *J* = 4.04 Hz, 2

H), 6.67 (s, 1 H), 7.16 (d, $J = 2.27$ Hz, 1 H), 7.28–7.34 (m, 1 H), 7.46 (t, $J = 8.97$ Hz, 1 H), 7.56 (dd, $J = 6.69, 2.65$ Hz, 1 H), 7.83 (d, $J = 2.02$ Hz, 1 H), 8.38 (s, 1 H), 9.47–9.51 (m, 1 H), 12.80 (s, 1 H). HPLC method 1: 100.0%, 4.85 min. HPLC method 2: 95.5%, 6.17 min.

N²-{8-Chloro-4-[(3-chloro-4-fluorophenyl)amino]-3-cyanoquinolin-6-yl}-N-pyridin-3-ylglycinamide (37). To a mixture of **36** (233 mg, 0.58 mmol), 3-aminopyridine (70 μ L, 0.70 mmol), and diisopropylethylamine (402 μ L, 2.31 mmol) in DMF (5 mL) was added BOP (301 mg, 0.68 mmol). After 2 h, the mixture was purified by HPLC to give **37** as a tan solid (129 mg, 54%). ¹H NMR (400 MHz, DMSO-*d*₆) δ ppm 4.15 (s, 2 H), 6.88 (s, 1 H), 7.17 (d, $J = 2.27$ Hz, 1 H), 7.24–7.30 (m, 1 H), 7.43 (t, $J = 8.97$ Hz, 1 H), 7.51 (dd, $J = 6.57, 2.53$ Hz, 1 H), 7.61–7.69 (m, 2 H), 8.22–8.28 (m, 1 H), 8.41–8.46 (m, 2 H), 8.97 (s, 1 H), 9.55 (s, 1 H), 10.56 (s, 1 H); HRMS calcd for C₂₃H₁₅Cl₂FN₆O + H⁺, 481.074 12, found (ESI-FTMS, [M + H]¹⁺), 481.0754. HPLC method 1: 97.4%, 4.37 min. HPLC method 2: 100.0%, 5.24 min.

General Procedure for the Synthesis of Imidazolecarbaldehydes 52–54. 4-Isopropyl-1H-imidazole-5-carbaldehyde (52). Sulfuryl chloride (5.3 mL, 9.0 g, 66 mmol) was added dropwise to ethyl isobutyrylacetate (10.2 mL, 10.0 g, 63.2 mmol) in 50 mL of CHCl₃ at 0 °C. The mixture was heated at reflux for 2 h and concentrated to give ethyl 2-chloro-4-methyl-3-oxopentanoate of sufficient purity to be used directly in the next step (12.2 g, 94% yield): ¹H NMR (400 MHz, CDCl₃) δ ppm 1.17 (dd, $J = 9.1, 6.8$ Hz, 6 H), 1.30 (t, $J = 6.8$ Hz, 3 H), 2.99–3.16 (m, 1 H), 4.24–4.33 (m, 2 H), 4.92 (s, 1 H). Ethyl 2-chloro-4-methyl-3-oxopentanoate (12.2 g, 63.3 mol) was reacted with formamide (25 mL, 29 g, 0.63 mol) and water (2.3 mL, 2.3 g, 0.13 mol). The crude product was purified by flash chromatography over silica gel (4–6% MeOH in CH₂Cl₂) to give ethyl 4-isopropyl-1H-imidazole-5-carboxylate of sufficient purity to be used in the next step (0.558 g, 4.8% yield): ¹H NMR (400 MHz, DMSO-*d*₆) δ ppm 1.20 (d, $J = 7.1$ Hz, 6 H), 1.23–1.33 (m, 3 H), 3.44–3.57 (m, 0.35 H), 3.65–3.79 (m, 0.65 H), 4.12–4.33 (m, 2 H), 7.58 (s, 0.65 H), 7.66 (s, 0.35 H), 12.39 (br s, 0.65 H), 12.67 (br s, 0.35 H). Ethyl 4-isopropyl-1H-imidazole-5-carboxylate (0.55 g, 3.0 mmol) in 20 mL of THF was reduced with a 1.0 M THF solution of LiAlH₄ (3.1 mL, 3.1 mmol). Workup gave (4-isopropyl-1H-imidazol-5-yl)methanol of sufficient purity to be used directly in the next step (0.39 g, 92% yield): ¹H NMR (400 MHz, DMSO-*d*₆) δ ppm 1.15 (d, $J = 6.8$ Hz, 6 H), 2.78–3.12 (m, 1 H), 4.33 (s, 2 H), 4.66 (br s, 1 H), 7.38 (s, 1 H), 11.66 (br s, 1 H). (4-Isopropyl-1H-imidazol-5-yl)methanol (0.21 g, 1.55 mmol) was oxidized with activated manganese dioxide (0.40 g, 4.64 mmol) in 5 mL of acetone. The crude product was purified by flash chromatography over silica gel (gradient elution, 5–100% EtOAc in CH₂Cl₂) to give pure **52** as a pale-pink solid (0.27 g, 37% yield): ¹H NMR (400 MHz, DMSO-*d*₆) δ ppm 1.23 (d, $J = 6.8$ Hz, 6 H), 3.41 (br s, 0.35 H), 3.53–3.68 (m, 0.65 H), 7.71 (s, 0.65 H), 7.85 (s, 0.35 H), 9.82 (s, 1 H), 12.66 (br s, 0.65 H), 12.91 (br s, 0.35 H).

8-Bromo-4-[(3-chloro-4-fluorophenyl)amino]-6-[(4-isopropyl-1H-imidazol-5-yl)methyl]amino}quinoline-3-carbonitrile (38). The procedure described above for the synthesis of **12** was followed, reacting **9d** (300 mg, 0.76 mmol) with **52** (106 mg, 0.76 mmol) and NaCNBH₃ (32 mg, 0.51 mmol) in 9 mL of THF and 3 mL of MeOH. The crude product was purified by HPLC and lyophilized to give **38** as a yellow solid (162 mg, 41% yield): ¹H NMR (400 MHz, DMSO-*d*₆) δ ppm 1.16 (d, $J = 6.8$ Hz, 6 H), 3.09 (br s, 1 H), 4.13 (s, 2 H), 6.49 (s, 1 H), 7.21 (s, 1 H), 7.24–7.33 (m, 1 H), 7.44 (t, $J = 9.0$ Hz, 1 H), 7.48–7.55 (m, 2 H), 7.83 (s, 1 H), 8.39 (s, 1 H), 9.45 (s, 1 H), 11.82 (s, 1 H); HRMS (ESI⁺) calcd for C₂₃H₂₀BrClFN₆ (MH⁺) 513.0600, found 513.0594. HPLC method 1: 99.3%, 4.46 min. HPLC method 2: 97.4%, 5.64 min. Anal. (C₂₃H₂₀BrClFN₆·H₂O): C, 51.94; H, 3.98; N, 15.80. Found: C, 51.92; H, 3.66; N, 15.35.

8-Chloro-4-[(3-chloro-4-fluorophenyl)amino]-6-[(5-isopropyl-1H-imidazol-4-yl)methyl]amino}quinoline-3-carbonitrile (39). The procedure described above for the synthesis of **12** was followed, reacting **9c** (76 mg, 0.22 mmol) with **52** (36 mg, 0.26 mmol) and

NaCNBH₃ (22 mg, 0.35 mmol) in 9 mL of EtOH. The crude product was purified by HPLC and lyophilized to give **39** as a yellow solid (74 mg, 72%): ¹H NMR (400 MHz, DMSO-*d*₆) δ ppm 1.16 (d, $J = 7.07$ Hz, 6 H), 4.16 (d, $J = 4.55$ Hz, 2 H), 6.54 (d, $J = 4.42$ Hz, 1 H), 7.19 (d, $J = 2.02$ Hz, 1 H), 7.26–7.34 (m, 1 H), 7.45 (t, $J = 8.97$ Hz, 1 H), 7.49–7.56 (m, 2 H), 7.61 (d, $J = 2.27$ Hz, 1 H), 8.16 (s, 1 H), 8.39 (s, 1 H), 9.47 (s, 1 H); HRMS (ESI⁺) calcd for C₂₃H₁₂Cl₂FN₆ (MH⁺) 469.110 50, found 469.1096. HPLC method 1: 98.8%, 4.37 min. HPLC method 2: 99.5%, 5.51 min.

8-Chloro-4-[(3-chloro-4-fluorophenyl)amino]-6-[(5-propyl-1H-imidazol-4-yl)methyl]amino}quinoline-3-carbonitrile (40). The imidazolecarbaldehyde **53** was prepared according to the general procedure described above for **52**. The procedure described above for the synthesis of **12** was then followed, reacting **9c** (80 mg, 0.23 mmol) with **53** (38 mg, 0.28 mmol) and NaCNBH₃ (17 mg, 0.28 mmol) in 9 mL of EtOH. The crude product was purified by HPLC and lyophilized to give **40** as a yellow solid (61 mg, 56%): ¹H NMR (400 MHz, DMSO-*d*₆) δ ppm 0.83 (t, $J = 7.45$ Hz, 3 H), 1.53 (q, 2 H), 4.15 (d, $J = 4.80$ Hz, 2 H), 6.27 (s, 1 H), 6.51 (d, 2 H), 7.18 (s, 1 H), 7.25–7.32 (m, 1 H), 7.45 (t, $J = 8.97$ Hz, 1 H), 7.49–7.54 (m, 2 H), 7.61 (s, 1 H), 8.16–8.20 (m, 1 H), 8.39 (s, 1 H), 9.46 (s, 1 H). HPLC method 1: 99.1%, 4.47 min. HPLC method 2: 99.8%, 5.70 min.

8-Chloro-4-[(3-chloro-4-fluorophenyl)amino]-6-[(5-ethyl-1H-imidazol-4-yl)methyl]amino}quinoline-3-carbonitrile (41). The imidazolecarbaldehyde **54** was prepared according to the general procedure described above for **42a**. The procedure described above for the synthesis of **12** was then followed, reacting **9c** (43 mg, 0.12 mmol) with **54** (15 mg, 0.12 mmol) and NaCNBH₃ (9 mg, 0.14 mmol) in 4 mL of EtOH. The reaction was concentrated and the residue was purified by HPLC to give **41** as a yellow solid (16 mg, 30%): ¹H NMR (400 MHz, DMSO-*d*₆) δ ppm 1.12 (t, $J = 7.58$ Hz, 3 H), 2.51–2.61 (m, 2 H), 4.16 (d, $J = 4.04$ Hz, 2 H), 6.54 (s, 2 H), 7.20 (s, 1 H), 7.26–7.33 (m, 1 H), 7.45 (t, $J = 9.22$ Hz, 1 H), 7.50–7.63 (m, 2 H), 8.14 (s, 1 H), 8.39 (s, 1 H), 9.48 (s, 1 H); HRMS calcd for C₂₂H₁₇Cl₂FN₆ + H⁺, 455.094 85, found (ESI-FTMS, [M + H]¹⁺), 455.0945. HPLC method 1: 96.9%, 4.28 min. HPLC method 2: 97.0%, 5.31 min.

Methyl 5-[(8-Bromo-4-[(3-chloro-4-fluorophenyl)amino]-3-cyanoquinolin-6-yl)amino]methyl-1H-imidazole-4-carboxylate (42). In a microwave vial, methyl 5-hydroxymethyl-1H-imidazole-4-carboxylate (0.20 g, 1.28 mmol) was dissolved in 2.5 mL each of CH₂Cl₂ and 1,4-dioxane, and activated MnO₂ (0.95 g, 11 mmol) was added. The vial was heated in a microwave reactor at 140 °C for 5 min. The contents of the vial were then rinsed into a 1 L flask and stirred with 400 mL of MeOH for 30 min. The suspension was then filtered to remove the deactivated MnO₂, and the filtrate was dried over anhydrous Na₂SO₄, filtered a second time, and evaporated to give methyl 5-formyl-1H-imidazole-4-carboxylate of sufficient purity to be used in the next step (163 mg, 83% yield): ¹H NMR (400 MHz, DMSO-*d*₆) δ ppm 3.88 (s, 3 H), 8.06 (s, 1 H), 10.22 (s, 1 H), 13.76 (s, 1 H); HRMS (ESI⁺) calcd for C₆H₇N₂O₃ (MH⁺) 155.0451, found 155.0450. The procedure described above for the synthesis of **12** was followed, reacting **9d** (400 mg, 1.02 mmol) with methyl 5-formyl-1H-imidazole-4-carboxylate (157 mg, 1.02 mmol) and NaCNBH₃ (43 mg, 0.68 mmol) in 12 mL of THF and 4 mL of MeOH. The crude product was purified by HPLC and lyophilized to give **42** as a bright-yellow powder (0.18 g, 33% yield): ¹H NMR (400 MHz, DMSO-*d*₆) δ ppm 3.76 (br s, 3 H), 4.50 (br s, 1 H), 4.62 (br s, 1 H), 6.65 (br s, 0.5 H), 6.74 (br s, 0.5 H), 7.20–7.31 (m, 2 H), 7.43 (t, $J = 9.0$ Hz, 1 H), 7.50 (dd, $J = 6.4, 2.7$ Hz, 1 H), 7.63–7.88 (m, 2 H), 8.39 (s, 1 H), 9.45 (br s, 1 H), 12.70 (br s, 0.5 H), 13.09 (br s, 0.5 H); HRMS (ESI⁺) calcd for C₂₂H₁₀BrClFN₆O₂ (MH⁺) 529.0185, found 529.0186. HPLC method 1: 99.1%, 4.98 min. HPLC method 2: 98.5%, 6.63 min.

8-Chloro-4-[(3-chloro-4-fluorophenyl)amino]-6-[(4-[3-(dimethylamino)propyl]-1H-imidazol-5-yl)methyl]amino}quinoline-3-carbonitrile (43). In a 50 mL round-bottomed flask were added **56** (355 mg, 1.04 mmol), *N,N*-dimethylprop-2-yn-1-amine (178 mg, 2.08 mmol), dichlorobis(triphenylphosphine)palladium (85 mg, 0.12

mmol), and triethylamine (800 mg, 7.89 mmol) in 5 mL of DMF. The mixture was heated to 90 °C for 2.5 h. 1-(Benzyloxymethyl)-4-(3-(dimethylamino)prop-1-ynyl)-1*H*-imidazole-5-carbaldehyde was obtained upon a standard EtOAc aqueous workup and was sufficiently pure for the next step. ¹H NMR (400 MHz, DMSO-*d*₆) δ ppm 2.25 (s, 6 H), 3.54 (s, 2 H), 4.54 (s, 2 H), 5.72 (s, 2 H), 7.23–7.37 (m, 5 H), 8.28 (s, 1 H), 9.86 (s, 1 H). Crude **57** was dissolved in THF (15 mL), and approximately 10 mg of 5% Pd on carbon was added. The mixture was hydrogenated in a Parr shaker apparatus at 50 psi for 3 h. After filtration through Celite, the solvent was removed under reduced pressure. ¹H NMR (400 MHz, DMSO-*d*₆) δ ppm 1.73–1.79 (m, 2 H), 2.16 (s, 6 H), 2.24–2.30 (m, 2 H), 2.78–2.84 (m, 2 H), 4.51 (s, 2 H), 5.71 (s, 2 H), 7.21–7.38 (m, 5 H), 8.13 (s, 1 H), 9.86 (s, 1 H). The crude material from the previous step was stirred in 10 mL of 6 N HCl and 10 mL of MeOH to give 4-(3-(dimethylamino)propyl)-1*H*-imidazole-5-carbaldehyde (**57**), which was immediately used as a solution in the next step. The procedure described above for the synthesis of **12** was followed, reacting **9c** (100 mg, 0.29 mmol) with a solution of **57** and NaCNBH₃ (21.0 mg, 0.33 mmol) at room temperature for 5 h. The mixture was concentrated and purified via preparative HPLC to give **43** as a yellow solid (98 mg, 66%): ¹H NMR (400 MHz, DMSO-*d*₆) δ ppm 1.64–1.74 (m, 2 H), 2.19 (s, 6 H), 2.29–2.36 (m, 2 H), 2.53–2.58 (m, 2 H), 4.17 (d, *J* = 4.04 Hz, 2 H), 6.57 (t, *J* = 4.42 Hz, 1 H), 7.21 (d, *J* = 2.27 Hz, 1 H), 7.25–7.33 (m, 1 H), 7.45 (t, *J* = 8.97 Hz, 1 H), 7.53 (q, *J* = 2.95 Hz, 1 H), 7.59 (d, *J* = 2.27 Hz, 1 H), 8.19 (s, 2 H), 8.39 (s, 1 H), 9.48–9.56 (m, 1 H); HRMS calcd for C₂₅H₂₄Cl₂FN₇ + H⁺, 512.152 70, found (ESI-FTMS, [M + H]⁺), 512.1522. HPLC method 1: 95.2%, 3.53 min. HPLC method 2: 95.1%, 3.01 min.

8-Bromo-4-[(3-chloro-4-fluorophenyl)amino]-6-[(1-methyl-1*H*-imidazol-4-yl)methyl]amino}quinoline-3-carbonitrile (44**).** (4-Ethyl-1*H*-imidazol-5-yl)methanol (1.00 g, 7.14 mmol) was dissolved in 20 mL of THF and cooled to 0 °C. A 1.0 M solution of LiAlH₄ in THF (7.1 mL, 7.1 mmol) was then added slowly via syringe. The reaction mixture allowed to warm to room temperature over 30 min and then cooled to 0 °C and quenched by addition of 10 mL of saturated Na₂SO₄ followed by addition of enough 1 M HCl to bring the solution to pH 8. The white precipitate was then filtered off and washed with EtOAc. The filtrate was dried, filtered, and evaporated to give (1-methyl-1*H*-imidazol-4-yl)methanol as a waxy yellow solid (0.80 g, 100% yield) of sufficient purity to be used in the next step. ¹H NMR (400 MHz, DMSO-*d*₆) δ ppm 3.60 (s, 3 H), 4.30 (s, 2 H), 4.79 (br s, 1 H), 6.92 (s, 1 H), 7.45 (s, 1 H). Crude (1-methyl-1*H*-imidazol-4-yl)methanol (0.81 g, 7.19 mmol) was stirred overnight at room temperature with activated manganese dioxide (1.87 g, 21.6 mmol) in 15 mL of acetone. The crude product was filtered through a pad of Celite and purified by flash chromatography over silica gel (10–100% EtOAc in CH₂Cl₂) to give pure 1-methyl-1*H*-imidazole-4-carbaldehyde as a waxy yellow solid (0.23 g, 30% yield): ¹H NMR (400 MHz, DMSO-*d*₆) δ ppm 3.73 (s, 3 H), 7.81 (s, 1 H), 8.00 (s, 1 H), 9.70 (s, 1 H). The procedure described above for the synthesis of **12** was followed, reacting **9d** (200 mg, 0.51 mmol) with 1-methyl-1*H*-imidazole-4-carbaldehyde (56 mg, 0.51 mmol) and NaCNBH₃ (22 mg, 0.34 mmol) in 6 mL of THF and 2 mL of MeOH. The yellow precipitate that appeared was collected by suction filtration, washed with MeOH, and dried under vacuum to give **44** as a yellow powder (155 mg, 63% yield): ¹H NMR (400 MHz, DMSO-*d*₆) δ ppm 3.60 (s, 3 H), 4.21 (d, *J* = 5.3 Hz, 2 H), 6.67 (t, *J* = 5.2 Hz, 1 H), 7.05 (s, 1 H), 7.23 (d, *J* = 2.3 Hz, 1 H), 7.28 (ddd, *J* = 8.7, 4.2, 2.8 Hz, 1 H), 7.45 (t, *J* = 9.0 Hz, 1 H), 7.52 (dd, *J* = 6.7, 2.7 Hz, 1 H), 7.54 (s, 1 H), 7.79 (d, *J* = 2.3 Hz, 1 H), 8.38 (s, 1 H), 9.47 (s, 1 H); HRMS (ESI⁺) calcd for C₂₁H₁₆BrClFN₆ (MH⁺) 485.0287, found 485.0278. HPLC method 1: 98.0%, 4.20 min. HPLC method 2: 96.6%, 4.90 min. Anal. (C₂₁H₁₆BrClFN₆·H₂O) C, H, N.

8-Chloro-4-(3-chloro-4-fluorophenylamino)-6-((2-ethyl-5-methyl-1*H*-imidazol-4-yl)methylamino)quinoline-3-carbonitrile (45**).** The procedure described above for the synthesis of **12** was followed, reacting **9c** (80 mg, 0.23 mmol) with 2-ethyl-5-methyl-1*H*-imidazole-4-carbaldehyde (67 mg, 0.49 mmol) and NaCNBH₃ (24

mg, 0.38 mmol) in 6 mL of EtOH. The crude product was purified by HPLC and lyophilized to give **45** as a tan solid (52 mg, 48%): ¹H NMR (400 MHz, DMSO-*d*₆) δ ppm 1.17 (t, *J* = 7.58 Hz, 3 H), 2.06–2.17 (m, 3 H), 2.51–2.60 (m, 2 H), 4.09 (d, *J* = 4.55 Hz, 2 H), 6.53 (t, *J* = 4.80 Hz, 1 H), 7.18 (t, *J* = 2.27 Hz, 1 H), 7.25–7.32 (m, 1 H), 7.45 (t, *J* = 8.97 Hz, 1 H), 7.52 (dd, *J* = 6.57, 2.78 Hz, 1 H), 7.60 (d, *J* = 2.27 Hz, 1 H), 8.16 (s, 1 H), 8.39 (s, 1 H), 9.47 (s, 1 H); HRMS (ESI⁺) calcd for C₂₃H₁₂Cl₂FN₆ (MH⁺) 469.110 50, found 469.1102. HPLC method 1: 97.1%, 4.28 min. HPLC method 2: 98.5%, 5.16 min. Anal. (C₂₃H₁₂Cl₂FN₆·H₂O·HCO₂H) C, H, N.

8-Chloro-4-[(3-chloro-4-fluorophenyl)amino]-6-[[2,5-dimethyl-1*H*-imidazol-4-yl)methyl]amino}quinoline-3-carbonitrile (46**).** The procedure described above for the synthesis of **12** was followed, reacting **9c** (80 mg, 0.23 mmol) with 2,4-dimethyl-1*H*-imidazole-5-carbaldehyde (34 mg, 0.28 mmol) and NaCNBH₃ (17 mg, 0.28 mmol) in 9 mL of EtOH. The product precipitated out of solution and was washed with EtOH to give **46** as a yellow solid (49 mg, 46%): ¹H NMR (400 MHz, DMSO-*d*₆) δ ppm 2.10 (s, 3 H), 2.19 (s, 3 H), 4.07 (m, 2 H), 6.51 (s, 1 H), 7.17 (s, 1 H), 7.24–7.30 (m, 1 H), 7.45 (t, *J* = 9.09 Hz, 1 H), 7.53 (d, *J* = 3.03 Hz, 1 H), 7.59 (s, 1 H), 8.14 (s, 1 H), 8.39 (s, 1 H), 9.45 (s, 1 H); HRMS, calcd for C₂₂H₁₇Cl₂FN₆ + H⁺, 455.094 85, found (ESI-FTMS, [M + H]⁺), 455.0947. HPLC method 1: 97.2%, 3.96 min. HPLC method 2: 95.3%, 3.68 min. Anal. (C₂₂H₁₇Cl₂FN₆·H₂O·HCO₂H) C, H, N.

8-Chloro-4-[(3-chloro-4-fluorophenyl)amino]-6-[[1-methyl-1*H*-imidazol-5-yl)methyl]amino}quinoline-3-carbonitrile (47**).** The procedure described above for the synthesis of **12** was followed, reacting **9c** (80 mg, 0.23 mmol) with 1-methyl-1*H*-imidazole-5-carbaldehyde (38 mg, 0.25 mmol) and NaCNBH₃ (17 mg, 0.28 mmol) in 9 mL of EtOH. The mixture was concentrated and the residue was purified via preparative HPLC and lyophilized to give **47** as a yellow solid (65 mg, 78%): ¹H NMR (400 MHz, DMSO-*d*₆) δ ppm 3.69 (s, 3 H), 4.39 (d, *J* = 5.05 Hz, 2 H), 6.78–6.88 (m, 1 H), 7.14 (s, 1 H), 7.25 (d, *J* = 2.02 Hz, 1 H), 7.27–7.34 (m, 1 H), 7.46 (t, *J* = 8.97 Hz, 1 H), 7.51–7.58 (m, 1 H), 8.00 (s, 1 H), 8.13 (s, 1 H), 8.42 (s, 1 H), 9.47 (s, 1 H); HRMS calcd for C₂₁H₁₅Cl₂FN₆ + H⁺, 441.079 20, found (ESI-FTMS, [M + H]⁺), 441.078 60. HPLC method 1: 99.4%, 4.15 min. HPLC method 2: 99.4%, 4.87 min.

8-Bromo-4-(3-chloro-4-fluorophenylamino)-6-((2-phenyl-1*H*-imidazol-5-yl)methylamino)quinoline-3-carbonitrile (48**).** The procedure described above for the synthesis of **12** was followed, reacting **9d** (300 mg, 0.76 mmol) with 2-phenyl-1*H*-imidazole-5-carbaldehyde (132 mg, 0.76 mmol) and NaCNBH₃ (32 mg, 0.51 mmol) in 9 mL of THF and 3 mL of MeOH. The crude product was purified by trituration with boiling EtOH and a second crop of crystals were collected from the filtrate to give **48** as a yellow solid (206 mg, 49% yield): ¹H NMR (400 MHz, DMSO-*d*₆) δ ppm 4.30 (d, *J* = 5.8 Hz, 2 H), 6.77 (t, *J* = 5.3 Hz, 1 H), 7.20 (s, 1 H), 7.26–7.35 (m, 3 H), 7.37–7.47 (m, 3 H), 7.53 (dd, *J* = 6.6, 2.8 Hz, 1 H), 7.81 (s, 1 H), 7.90 (d, *J* = 7.3 Hz, 2 H), 8.37 (s, 1 H), 9.49 (s, 1 H), 11.94 (s, 0.5 H), 12.40 (s, 0.5 H); HRMS (ESI⁺) calcd for C₂₆H₁₈BrClFN₆ (MH⁺) 547.0444, found 547.0457. HPLC method 1: 100.0%, 4.34 min. HPLC method 2: 98.3%, 5.14 min.

8-Bromo-4-[(3-chloro-4-fluorophenyl)amino]-6-[[1-(2-morpholin-4-ylethyl)-1*H*-imidazol-4-yl)methyl]amino}quinoline-3-carbonitrile (49**).** In a sealable pressure tube was added 1*H*-imidazole-4-carbaldehyde (750 mg, 7.8 mmol), sodium carbonate (827 mg, 7.8 mmol), sodium iodide (585 mg, 3.9 mmol), 4-(2-chloroethyl)morpholine hydrochloride (726 mg, 3.9 mmol), and 10 mL of DMF under a stream of nitrogen gas. The tube was then sealed and heated to 100 °C overnight. The mixture was allowed to cool to room temperature, filtered, and diluted with EtOAc. The EtOAc layer was extracted twice with brine, and the aqueous phase was back-extracted with EtOAc. The organic layers were combined, dried over MgSO₄, and filtered and concentrated under reduced pressure. The substituted aldehyde was used without further purification.

The procedure described above for the synthesis of **12** was followed using **9d** (150 mg, 0.38 mmol) with crude 1-(2-

morpholinoethyl)-1*H*-imidazole-4-carbaldehyde and NaCNBH₃ (35 mg, 0.56 mmol) in 10 mL of EtOH. The mixture was concentrated and the residue was purified by HPLC and lyophilized to give **49** as a yellow solid (40 mg, 18%): ¹H NMR (400 MHz, MeOD) δ ppm 2.36–2.45 (m, 4 H), 2.64 (t, 2 H), 3.52–3.59 (m, 4 H), 4.08 (t, *J* = 6.19 Hz, 2 H), 4.33 (s, 2 H), 7.11 (d, *J* = 1.01 Hz, 1 H), 7.14 (d, *J* = 1.26 Hz, 1 H), 7.17–7.25 (m, 1 H), 7.28 (t, *J* = 8.84 Hz, 1 H), 7.40 (dd, *J* = 6.82, 2.02 Hz, 1 H), 7.67 (d, *J* = 1.01 Hz, 2 H), 8.29 (s, 1 H), 8.39 (s, 1 H); HRMS (ESI⁺) calcd for C₂₆H₂₄BrClFN₇O (MH⁺) 584.097 10, found 584.097. HPLC method 1: 98.4%, 3.54 min. HPLC method 2: 100.0%, 3.62 min.

8-Bromo-4-[(3-chloro-4-fluorophenyl)amino]-6-[[1-[2-(methylsulfonyl)ethyl]-1*H*-imidazol-4-yl]methyl]amino]quinoline-3-carbonitrile (50). In a microwave tube was added methyl vinyl sulfone (264 mg, 5.0 mmol), 1*H*-imidazole-5-carbaldehyde (160 mg, 1.67 mmol), and 4 mL of DMF. The mixture was reacted in a microwave reactor at 150 °C for 1 h. The reaction mixture was concentrated to give 1-(2-(methylsulfonyl)ethyl)-1*H*-imidazole-4-carbaldehyde. The procedure described above for the synthesis of **12** was followed, reacting **9d** (340 mg, 0.87 mmol) with 1-(2-(methylsulfonyl)ethyl)-1*H*-imidazole-4-carbaldehyde and NaCNBH₃ (30 mg, 0.48 mmol) in 10 mL of EtOH. The reaction mixture was concentrated and the residue was purified by HPLC and lyophilized to give **50** as a yellow solid (90 mg, 18%): ¹H NMR (400 MHz, DMSO-*d*₆) δ ppm 2.84 (s, 3 H), 3.64 (t, *J* = 6.95 Hz, 2 H), 4.23 (d, *J* = 4.80 Hz, 2 H), 4.36 (t, *J* = 6.95 Hz, 2 H), 6.70 (t, *J* = 5.43 Hz, 1 H), 7.20 (s, 1 H), 7.24 (d, *J* = 2.02 Hz, 1 H), 7.25–7.32 (m, 1 H), 7.45 (t, *J* = 9.09 Hz, 1 H), 7.52 (dd, *J* = 6.57, 2.78 Hz, 1 H), 7.68 (d, *J* = 1.26 Hz, 1 H), 7.79 (d, *J* = 2.27 Hz, 1 H), 8.14 (s, 1 H), 8.38 (s, 1 H), 9.47 (s, 1 H); HRMS (ESI⁺) calcd for C₂₃H₁₉BrClFN₆O₂S (MH⁺) 577.021 89, found 577.0225. HPLC method 1: 98.7%, 4.25 min. HPLC method 2: 100.0%, 4.96 min.

8-Bromo-4-[(3-chloro-4-fluorophenyl)amino]-6-[(2*H*-1,2,3-triazol-4-yl)methyl]amino]quinoline-3-carbonitrile (51). In a microwave vial were added 3,3-diethoxyprop-1-yne (1.0 g, 7.5 mmol), 1,2-diethoxyethane (15 mL), and tributyltin azide (3.2 g, 9.76 mmol). The sealed vial was heated in a microwave reactor at 180 °C for 3 h. The solvent was evaporated, and the residue was treated with 2 M HCl in MeOH for 16 h. The solvent was evaporated, and the residue was dissolved in methanol (10 mL) and dichloroethane (10 mL). To this was added **9d** (500 mg, 1.3 mmol). Acetic acid was added to bring the pH of the solution to 4, and the mixture was stirred for 15 min. Sodium triacetoxyborohydride (542 mg, 2.55 mmol) was then added, and the mixture was stirred at room temperature overnight. The reaction mixture was evaporated to dryness and the residue was purified via preparative HPLC and lyophilized to give **51** as a yellow solid (151 mg, 24%). ¹H NMR (400 MHz, MeOD) δ ppm 4.54 (s, 2 H), 7.18 (d, *J* = 2.53 Hz, 1 H), 7.21–7.31 (m, 2 H), 7.41 (dd, *J* = 6.44, 2.40 Hz, 1 H), 7.69 (d, *J* = 2.27 Hz, 2 H), 8.30 (s, 1 H); HRMS (ESI⁺) calcd for C₁₉H₁₂BrClFN₇ (MH⁺) 472.0090, found 472.0030. HPLC method 1: 100.0%, 5.01 min. HPLC method 2: 98.9%, 6.26 min

8-Bromo-4-(3-chloro-4-fluorophenylamino)-6-((1-(3-(dimethylamino)propyl)-1*H*-1,2,3-triazol-4-yl)methylamino]quinoline-3-carbonitrile (55). In a 15 mL round-bottomed flask were added **9d** (40 mg, 0.10 mmol), dichloroethane (2 mL), and 1-(3-(dimethylamino)propyl)-1*H*-1,2,3-triazole-4-carbaldehyde (24 mg, 0.12 mmol). The mixture was stirred for 15 min. Sodium triacetoxyborohydride (55 mg, 0.27 mmol) was then added, and the mixture was stirred at room temperature for 5 h. The reaction mixture was evaporated to dryness and the residue was purified via preparative HPLC and lyophilized to give the product as a yellow solid (42 mg, 75%). ¹H NMR (400 MHz, MeOD) δ ppm 2.36–2.54 (m, 2 H), 2.94 (s, 6 H), 3.18–3.29 (m, 2 H), 4.60–4.69 (m, 4 H), 7.33 (d, *J* = 2.27 Hz, 1 H), 7.35–7.46 (m, 2 H), 7.56 (dd, *J* = 6.44, 2.40 Hz, 1 H), 7.81 (d, *J* = 2.27 Hz, 1 H), 8.11 (s, 1 H), 8.43 (s, 1 H), 8.50 (s, 1 H). HPLC method 1: 94.2%, 4.31 min. HPLC method 2: 96.7%, 5.27 min.

Biology. For a complete description of the in vitro Tpl2 and TNF-α assays, see ref 18.

In Vitro Kinase Selectivity Assays. Scintiplate (³³P) assays were used to measure the activities of PKA (Panvera), PKC (Panvera), S6K (Upstate), JNK1 (Upstate), and MK2 41-400 (in house). The kinase reactions were performed at room temperature in streptavidin-coated Scintiplate (Perkin-Elmer) with a 100 μL/well reaction mixture, which contains the compounds in 1% DMSO, 20 mM HEPES, pH7.5, 10 mM MgCl₂, 4.5 mM DTT, 0.01% Triton X100, 3 μM ATP, 1.3 nM [^γ-³³P]ATP, and 200 nM substrate peptide. All assays were initiated by adding an ATP/peptide mixture. The reaction time was 10 min for PKA, 30 min for PKC, 80 min for S6K, 90 min for Jnk1, and 20 min for MK2 41-400. Reactions were terminated with 50 μL of 0.5 M EDTA. Plates were washed with PBS/0.05% Tween-20 six times and read on a MicroBeta TriLux reader (Perkin-Elmer).

The peptide substrates used were biotin-GRTGRRNSI for PKA/PKCα, biotin-RRRLSSLRA for S6K, biotin-ATF2 (19-96) (Upstate) for JNK1, and biotin-RTPKLARQASIELPSM for MK2. ELISA was used to measure the activities of p38 (in house), Src (Upstate), CAMKII (Upstate), and IKKβ (Upstate). The kinase reactions were performed at room temperature on streptavidin-coated plates (Sigma) or Anti-GST (Amersham) coated Maxisorp plates (Nunc) with 100 μL/well reaction mixture (same as for the Scintiplate assays but without [^γ-³³P]ATP). All assays were initiated with the ATP/substrate mixture. The reaction time was 60 min. Reactions were terminated with 50 μL of 0.5 M EDTA. Plates were washed with PBS/0.05% Tween-20 six times. Detection antibodies in antibody dilution buffer (10 mM MOPS 7.5, 150 mM NaCl, 0.05% Tween-20, 0.1% gelatin, 0.02% NaN₃, 1% BSA) were added into plates and incubated for 60 min at ambient temperature, and then plates were washed again. Enhancement buffer (Perkin-Elmer) (100 μL/well) was added to the plates, and the samples were incubated for 10 min. Read Plates were read using a VictorII plate reader (Perkin-Elmer).

The peptide substrates were biotin-QSTKVPQTPLHTSRVL for p38, biotin-KKEGPWLEEEEEAYGWMDF for Src, and biotin-RTPKLARQASIELPSM for CAMKII/IKKβ. Detection antibodies were p38, anti-P-MK2 (in house), 1:4000, and DELFIA Eu-N1 goat anti-rabbit-IgG, 1:2000; Src, P-Tyr-100 (Cell Signaling), 1:1000, and DELFIA Eu-N1 rabbit antimouse-IgG (Perkin-Elmer), 1:1000; CAMKII and IKKβ, anti-P-LSP1 (in house), 1:10000, and DELFIA Eu-N1 goat antirabbit-IgG, 1:5000.

Pharmacokinetic Studies. The animals used in the pharmacokinetic (PK) studies were male adult Sprague-Dawley rats (Charles River Laboratories, Wilmington, MA). All PK studies were performed at Wyeth Research Laboratories (Andover, MA) under the supervision of the Institutional Animal Care and Use Committee. The dose formulation for intravenous administration was 50% DMSO/50% polyethylene glycol 200 (PEG 200, v/v, 1 mL/kg). The oral dose formulation was an aqueous suspension containing 2% polysorbate 80 (aka Tween-80), 0.5% methylcellulose, and 0.06% lactic acid. Blood samples of approximately 0.25 mL were collected into K₂EDTA coated sampling tubes at 0.083, 0.25, 0.5, 1, 2, 4, 7, and 24 h after dose administration. Plasma samples were harvested and stored at -80 °C until analysis.

In a 0.5 mL 96-well plate, 50 μL of plasma sample was precipitated with 100 μL of acetonitrile containing 500 ng/mL internal standard. The internal standard is a compound with similar chemical structure as the test article. The samples were vortexed and centrifuged at 5700 rpm for 10 min. Supernatants were subjected to LC-MS/MS analysis. HPLC separation was performed on a Perkin-Elmer series 200 HPLC system (Perkin-Elmer, Norwalk, CT) using an XTerra MS C18 column (2.1 mm × 20 mm, 2.5 μm; Waters, Milford, MA). The detection of test articles was performed on a PESCIX API-3000 triple quadrupole mass spectrometer (Applied Biosystems, Concord, Ontario, L4K4V8, Canada) using TurboIon Spray source. Plasma standard curves were generated by plotting the peak area ratio of test article and internal standard against nominal concentrations.

The pharmacokinetic parameters were determined using WinNonlin (version 4.1, Pharsight, Mountain View, CA). Calculations were performed using the noncompartmental analysis approach. The

estimation of area under the plasma concentration versus time curve (AUC) was based on the log trapezoidal rule. The terminal rate constant (λ) was derived from the slope of the terminal log-linear phase of plasma concentration–time curves. The apparent terminal half-life ($t_{1/2}$) was calculated as $0.693/\lambda$. No statistical analysis other than descriptive statistics was conducted.

LPS-Induced Acute TNF- α Production in Rats. Jugular vein cannulated female Sprague-Dawley rats, 200 g, were obtained from Taconic Farms (Germantown, NY). The animals were fed food and water ad libitum, and all procedures were approved by the Institutional Animal Care and Use Committee. The compound was administered orally at 10 and 50 mg/kg. One hour later, the rats were challenged with LPS, administered intravenously (iv) at 1 mg/kg. Blood was drawn 10 and 90 min after the LPS challenge, and plasma was separated and stored at $-70\text{ }^{\circ}\text{C}$ until testing. The plasma concentration of the compound was determined in samples collected 10 and 90 min after the LPS challenge, while TNF- α concentration was determined in samples collected at 90 min after the challenge, using a mouse cytometric bead assay kit (CBA) obtained from BD Pharmingen (San Jose, CA). Mouse CBA kit detects rat TNF- α because of cross-reactivity of anti-TNF- α antibodies.

In Vitro Microsomal Metabolic Stability and Metabolism. Microsomes purchased from commercial vendors, such as In Vitro Technologies (Baltimore, MD) or Xenotech (Kansas City, KS), or microsomes prepared by differential ultracentrifugation utilizing the method described by Lake³⁵ were used. Microsomal protein and cytochrome P450 content were determined by the methods of Bradford³⁶ and Omura and Sato,³⁷ respectively. For human liver microsomes, the activities of major cytochrome P450 enzymes (i.e., CYP3A4, CYP2D6, and CYP2C9) were provided by the vendor or determined in-house. Microsomes were stored at $-80\text{ }^{\circ}\text{C}$ in aliquots (e.g., 200 μL) until use. Microsomes were pooled from at least three animals or subjects. The incubation mixture (prior to the addition of NADPH) was preincubated with the test compound for approximately 5 min at $37\text{ }^{\circ}\text{C}$, and the reaction was started by the addition of NADPH. Control incubations were performed in the absence of NADPH. Incubations were conducted for up to 1 h. An aliquot (e.g., 200 μL) of the incubation mixture was removed at zero time and at different time intervals (e.g., 10, 20, 30, and 60 min) to determine the time course of drug disappearance. Microsomal protein was precipitated with an organic solvent such as acetonitrile (2–3 volumes), and the drug and metabolites were extracted. The amount of unchanged drug remaining was determined by HPLC or LC/MS using an appropriate internal standard. An appropriate positive control, such as midazolam for CYP3A4, was included to assess interday and interlaboratory variations. For determination of metabolite profiles, the study was performed similarly to procedures described above with the exception that a higher substrate concentration (e.g., 10 μM or above) and an incubation time of at least 30 min were used to maximize the amounts of metabolites that were produced and characterized. For metabolic stability studies, peak area or peak height ratios (i.e., peak area/height of unchanged drug/peak area/height of internal standard) at each time point were used to determine the amount of unchanged drug, which was converted to the percentage of drug remaining using the peak area/height ratio values at zero time as 100%. The rate of drug disappearance was expressed as $\text{nmol min}^{-1}\text{ mg}^{-1}$ or $\text{pmol min}^{-1}\text{ mg}^{-1}$ protein based on the first 5 or 10 min of incubation and assuming linearity. The log of the percentage of the drug remaining (y -axis) was plotted against incubation time (x -axis). The slope from the linear regression line equals $-k$, and the in vitro $t_{1/2}$ equals $-0.693/k$.

Acknowledgment. The authors thank Drs. Tarek Mansour, Dennis Powell, John Potoski, and Allan Wissner for support, discussions, and advice; Drs. Pingzhong Huang and William Hallett for the large-scale preparation of intermediates; and Dr. Nelson Huang, Ms. Ning Pan, and Dr. Walter Masefski for analytical support.

Supporting Information Available: Elemental analysis data for compounds **11**, **18**, **33**, **38**, and **44–47**, quantitative pharmacological data for Figure 3 (TNF- α levels and plasma concentrations of **44** in individual animals), and experimental details for solubility and permeability measurements. This material is available free of charge via the Internet at <http://pubs.acs.org>.

References

- (1) Choy, E. H. S.; Panayi, G. S. P. Cytokine pathways and joint inflammation in rheumatoid arthritis. *N. Engl. J. Med.* **2001**, *344*, 907–916.
- (2) Feldmann, M.; Brennan, F. M.; Foxwell, B. M.; Maini, R. N. The role of TNF- α and IL-1 in rheumatoid arthritis. *Curr. Dir. Autoimmun.* **2001**, *3*, 188–199.
- (3) Feldmann, M.; Maini, R. N. Anti-TNF- α therapy of rheumatoid arthritis: What have we learned? *Ann. Rev. Immunol.* **2001**, *19*, 163–178.
- (4) Zhang, Y.; Xu, J.; Levin, J.; Hegen, M.; Li, G.; Robertshaw, H.; Brennan, F.; Cummons, T.; Clarke, D.; Vansell, N.; Nickerson-Nutter, C.; Barone, D.; Mohler, K.; Black, R.; Skotnicki, J.; Gibbons, J.; Feldmann, M.; Frost, P.; Larsen, G.; Lin, L.-L. Identification and characterization of 4-[[4-(2-butyloxy)phenyl]sulfonyl]-*N*-hydroxy-2,2-dimethyl-(3*S*)-thiomorpholinecarboxamide (TMI-1), a novel dual tumor necrosis factor- α -converting enzyme/matrix metalloproteinase inhibitor for the treatment of rheumatoid arthritis. *J. Pharmacol. Exp. Ther.* **2004**, *309*, 348–355.
- (5) Jarvis, B.; Faulds, D. Etanercept: a review of its use in rheumatoid arthritis. *Drugs* **1999**, *57*, 945–966.
- (6) Maini, R.; St. Clair, E. W.; Breedveld, F.; Furst, D.; Kalden, M.; Weisman, J.; Smolen, M.; Emery, P.; Harriman, G.; Feldmann, M.; Lipsky, P. Infliximab (chimeric anti-tumour necrosis factor alpha monoclonal antibody) versus placebo in rheumatoid arthritis patients receiving concomitant methotrexate: a randomised phase III trial. ATTRACT Study Group. *Lancet* **1999**, *354*, 1932–1939.
- (7) Kumar, S.; Boehm, J.; Lee, J. C. p38 MAP kinases: key signaling molecules as therapeutic targets for inflammatory diseases. *Nat. Rev. Drug Discovery* **2003**, *2*, 717–726.
- (8) Pargellis, C.; Tong, L.; Churchill, L.; Cirillo, P. F.; Gilmore, T.; Graham, A. G.; Grob, P. M.; Hickey, E. R.; Moss, N.; Pav, S.; Regan, J. Inhibition of p38 MAP kinase by utilizing a novel allosteric binding site. *Nat. Struct. Biol.* **2002**, *9*, 268–272. Salituro, F. G.; Bemis, G. W.; Germann, U. A.; Duffy, J. P.; Galullo, V. P.; Gao, H.; Harrington, E. M.; Wilson, K. P.; Su, M. S. Discovery of VX-745: A Novel, Orally Bioavailable and Selective p38 MAP Kinase Inhibitor. Presented at the 27th National Medicinal Chemistry Symposium, Kansas City, MO, 2000.
- (9) Lee, R. L.; Dominguez, C. MAP kinase p38 inhibitors: clinical results and an intimate look at their interactions with p38 α protein. *Curr. Med. Chem.* **2005**, *12*, 2979–2994.
- (10) Sasai, H.; Higashi, T.; Nakamori, S.; Miyoshi, J.; Suzuki, F.; Nomura, T.; Kakunaga, T. Syrian hamster embryo cell lines useful for detecting transforming genes in mouse tumours: detection of transforming genes in X-ray-related mouse tumours. *Br. J. Cancer* **1993**, *67*, 262–267.
- (11) Dumitru, C. D.; Ceci, J. D.; Tsatsanis, C.; Konoyiannis, D.; Stamatakis, K.; Lin, J. H.; Patriotic, C.; Jenkins, N. A.; Copeland, N. G.; Kollias, G.; Tschlis, P. N. TNF- α induction by LPS is regulated posttranscriptionally via a Tpl2/ERK-dependent pathway. *Nat. Med.* **2003**, *9*, 61–67.
- (12) Eliopoulos, A. G.; Dumitru, C. D.; Wang, C. C.; Cho, J.; Tschlis, P. N. Induction of COX-2 by LPS in macrophages is regulated by Tpl2-dependent CREB activation signals. *EMBO J.* **2002**, *21*, 4831–4840.
- (13) Dumitru, C. D.; Ceci, J. D.; Tsatsanis, C.; Konoyiannis, D.; Stamatakis, K.; Lin, J. H.; Patriotic, C.; Jenkins, N. A.; Copeland, N. G.; Kollias, G.; Tschlis, P. N. TNF- α induction by LPS is regulated posttranscriptionally via a Tpl2/ERK-dependent pathway. *Cell* **2000**, *103*, 1071–1083.
- (14) Lin, X.; E. T.; Cunningham, E. T., Jr.; Mu, Y.; Gelzinis, R.; Greene, W. C. The proto-oncogene *Cot* kinase participates in CD3/CD28 induction of NF- κ B acting through the NF- κ B-inducing kinase and I κ B kinases. *Immunity* **1999**, *10*, 271–280.
- (15) Chiarello, M.; Marinissen, M. J.; Gutkind, J. S. Multiple mitogen-activated protein kinase signaling pathways connect the *Cot* oncoprotein to the *c-jun* promoter and to cellular transformation. *Mol. Cell. Biol.* **2000**, *20*, 1747–1758.
- (16) Salmeron, A.; Ahmad, T. B.; Carlile, G. W.; Pappin, D.; Narsimhan, R. P.; Ley, S. Activation of MEK-1 and SEK-1 by Tpl-2 proto-oncoprotein, a novel MAP kinase kinase kinase. *EMBO J.* **1996**, *15*, 817–826.

- (17) Luciano, B. S.; Hsu, S.; Channavajhala, P. L.; Lin, L.-L.; Cuzzo, J. W. Phosphorylation of threonine 290 in the activation loop of Tpl2/Cot is necessary but not sufficient for kinase activity. *J. Biol. Chem.* **2004**, *279*, 52117–52123.
- (18) Gavrin, L. K.; Green, N.; Hu, Y.; Janz, K.; Kaila, N.; Li, H.-Q.; Tam, S. Y.; Thomason, J. R.; Gopalsamy, A.; Ciszewski, G.; Cuzzo, J. W.; Hall, J. P.; Hsu, S.; Telliez, J.-B.; Lin, L.-L. Inhibition of Tpl2 kinase and TNF- α production with 1,7-naphthyridine-3-carbonitriles: synthesis and structure–activity relationships. *Bioorg. Med. Chem. Lett.* **2005**, *15*, 5288–5292.
- (19) Hu, Y.; Green, N.; Gavrin, L. K.; Janz, K.; Kaila, N.; Li, H.-Q.; Thomason, J. R.; Cuzzo, J. W.; Hall, J. P.; Hsu, S.; Nickerson-Nutter, C.; Telliez, J.-B.; Lin, L.-L.; Tam, S. Y. Inhibition of Tpl2 kinase and TNF- α production with quinoline-3-carbonitriles for the treatment of rheumatoid arthritis. *Bioorg. Med. Chem. Lett.* **2006**, *16*, 6067–6072.
- (20) Part of this work has been presented: Green, N.; Guler, S.; Hotchandani, R.; Hu, Y.; Janz, K.; Kaila, N.; Li, H.-Q.; Thomason, J.; Tam, S.; Wu, J.; Joseph-McCarthy, D.; Cuzzo, J.; Hall, J. P.; Lin, L.-L. Selective Inhibition of Tpl2 Kinase and TNF Production with Quinoline-3-carbonitriles for the Treatment of Rheumatoid Arthritis. Presented at the 14th International Conference of the Inflammation Research Association, Cambridge, MD, October 15–19, 2006; SA33.
- (21) Wissner, A.; Overbeek, E.; Reich, M. F.; Floyd, M. B.; Johnson, B. D.; Mamuya, N.; Rosfjord, E. C.; Discafani, C.; Davis, R.; Shi, X.; Rabindran, S. K.; Gruber, B. C.; Ye, F.; Hallett, W. A.; Nilakantan, R.; Shen, R.; Wang, Y.-F.; Greenberger, L. M.; Tsou, H.-R. Synthesis and structure–activity relationships of 6,7-disubstituted 4-anilinoquinoline-3-carbonitriles. The design of an orally active, irreversible inhibitor of the tyrosine kinase activity of the epidermal growth factor receptor (EGFR) and the human epidermal growth factor receptor-2 (HER-2). *J. Med. Chem.* **2003**, *46*, 49–63 and references cited therein.
- (22) Testaferri, L.; Tingoli, M.; Tiecco, M. A convenient synthesis of aromatic thiols from unactivated aryl halides. *Tetrahedron Lett.* **1980**, *21*, 3099–3100.
- (23) Hirai, K.; Koike, H.; Ishiba, T.; Ueda, S.; Makino, I.; Yamada, H.; Ichihashi, T.; Mizushima, Y.; Ishikawa, M.; Ishihara, Y.; Hara, Y.; Hirose, H.; Shima, N.; Doteuchi, M. Amino acid amides of 2-[(2-aminobenzyl)sulfinyl]benzimidazole as acid-stable prodrugs of potential inhibitors of H⁺/K⁺ ATPase. *Eur. J. Med. Chem.* **1991**, *26*, 143–158.
- (24) Mohamadi, F.; Spees, M. M.; Staten, G. S.; Marder, P.; Kipka, J. K.; Johnson, D. A.; Boger, D. L.; Zarrinmayeh, H. Total synthesis and biological properties of novel antineoplastic (chloromethyl)-furanoidolines: an asymmetric hydroboration mediated synthesis of the alkylation subunits. *J. Med. Chem.* **1994**, *37*, 232–239.
- (25) Grunewald, G. L.; Vidyadhar, M.; Pazhenchevsky, M.; Pleiss, M. A.; Sall, D. J.; Seibel, W. L.; Reitzle, T. J. Synthesis of conformationally defined analogues of norfenfluramine. A highly stereospecific synthesis of amines from alcohols in the benzobicyclo[2.2.1]heptene system. *J. Org. Chem.* **1983**, *48*, 2321–2327.
- (26) Kim, D.-I.; Kim, H.-Y.; Kwon, L.-S.; Park, S.-D.; Jeon, G.-H.; Jung, K.-Y.; Min, J.-K.; Nam, W.-H.; Lee, K.; Chung, Y.-S.; Tanabe, S.; Kozono, T. Synthesis and biological activity of KCB-328 and its analogues: novel class III antiarrhythmic agents with little reverse frequency dependence. *Bioorg. Med. Chem. Lett.* **1999**, *9*, 85–90.
- (27) Standard reductive amination conditions were employed in most cases. See Experimental Section and ref 19 for specific examples.
- (28) Kiddle, J. J. Microwave irradiation in organophosphorus chemistry. Part 2: synthesis of phosphonium salts. *Tetrahedron Lett.* **2000**, *41*, 1339–1341.
- (29) Treccourt, F.; Breton, G.; Bonnet, V.; Mongin, F.; Marsais, F.; Queguiner, G. New syntheses of substituted pyridines via bromine–magnesium exchange. *Tetrahedron* **2000**, *56*, 1349–1360.
- (30) Paul, R.; Brockman, J. A.; Hallett, W. A.; Hanifin, J. W.; Tarrant, M. E.; Torley, L. W.; Callahan, F. M.; Fabio, P. F.; Johnson, B. D.; Lenhard, R. H.; Schaub, R. E.; Wissner, A. Imidazo[1,5-d][1,2,4]-triazines as potential antiasthma agents. *J. Med. Chem.* **1985**, *28*, 1704–1716.
- (31) Groziak, M. P.; Wei, L. Regioselective formation of imidazol-2-yllithium, imidazol-4-yllithium, and imidazol-8-yllithium species. *J. Org. Chem.* **1991**, *56*, 4296–4300.
- (32) For examples of this widely used approach, see refs 10 and 11 cited in ref 19.
- (33) Stamos, J.; Sliwkoski, M. X.; Eigenbrot, C. Structure of the epidermal growth factor receptor kinase domain alone and in complex with a 4-anilinoquinazoline inhibitor. *J. Biol. Chem.* **2002**, *277*, 46265–46272.
- (34) An example of this strategy: Hennequin, L. F.; Allen, J.; Breed, J.; Curwen, J.; Fennell, M.; Green, T. P.; Lambert-van der Brempt, C.; Morgentin, R.; Norman, R. A.; Olivier, A.; Otterbein, L.; Ple, P. A.; Warin, N.; Costello, G. *N*-(5-Chloro-1,3-benzodioxol-4-yl)-2-[2-(4-methylpiperazin-1-yl)ethoxy]-5-(tetrahydro-2H-pyran-4-yloxy)quinazolin-4-amine, a novel, highly selective, orally available, dual-specific c-Src/Abl kinase inhibitor. *J. Med. Chem.* **2006**, *49*, 6465–6488.
- (35) Lake, B. Preparation and characterization of microsomal fractions for studies on xenobiotic metabolism. In *Biochemical Toxicology: A Practical Approach*; Snell, K., Mullock, B., Eds.; IRL Press: Oxford, U.K., 1987; pp 183–215.
- (36) Bradford, M. M. A rapid and sensitive method for the quantitation of microgram quantities of protein utilizing the principle of protein–dye binding. *Anal. Biochem.* **1976**, *72*, 248–254.
- (37) Omura, T.; Sato, R. The carbon-monoxide binding pigment of liver microsomes. *J. Biol. Chem.* **1964**, *239*, 2370–2378.
- (38) Friesner, R. A.; Banks, J. L.; Murphy, R. B.; Halgren, T. A.; Klicic, J. J.; Mainz, D. T.; Repasky, M. P.; Knoll, E. H.; Shelley, M.; Perry, J. K.; Shaw, D. E.; Francis, P.; Shenkin, P. S. Glide: a new approach for rapid, accurate docking and scoring. 1. Method and assessment of docking accuracy. *J. Med. Chem.* **2004**, *47*, 1739–1749.
- (39) Halgren, T. A.; Murphy, R. B.; Friesner, R. A.; Beard, H. S.; Frye, L. L.; Pollard, W. T.; Banks, J. L. Glide: a new approach for rapid, accurate docking and scoring. 2. Enrichment factors in database screening. *J. Med. Chem.* **2004**, *47*, 1750–1759.
- (40) Miranker, A.; Karplus, M. Functionality maps of binding sites: a multiple copy simultaneous search method. *Proteins* **1991**, *11*, 29–34.
- (41) Evensen, E.; Joseph-McCarthy, D.; Karplus, M. *MCSSv2*, version 2.1; Harvard University: Cambridge, MA.
- (42) (a) Kerns, E. H.; Di, L. Pharmaceutical profiling in drug discovery. *Drug Discovery Today* **2003**, *8*, 316–323. (b) Avdeef, A.; Voloboy, D.; Foreman, A. Dissolution–Solubility of Multiprotic Drugs: pH, Buffer, Salt, Dual-Solid, and Aggregation Effects. In *ADME-TOX Approaches*; Testa, B., van de Waterbeemd, H., Eds.; Comprehensive Medicinal Chemistry II, Vol. 5; Elsevier: Oxford, U.K., 2006; pp 399–423. (c) Avdeef, A.; Testa, B. Physicochemical profiling in drug research: a brief state-of-the-art of experimental techniques. *Cell. Mol. Life Sci.* **2003**, *59*, 1681–1689. (d) Avdeef, A.; Bendels, S.; Di, L.; Faller, B.; Kansy, M.; Sugano, K.; Yamauchi, Y. PAMPA—a useful tool in drug discovery. *Eur. J. Pharm. Sci.*, in press. (e) Kansy, M.; Avdeef, A.; Fischer, H. Advances in screening for membrane permeability: high-resolution PAMPA for medicinal chemists. *Drug Discovery Today: Technol.* **2005**, *1*, 349–355. (f) Ruell, J. A.; Avdeef, A. Absorption Using the PAMPA Approach. In *Optimization in Drug Discovery: In Vitro Methods*; Yan, Z.; Caldwell, G.W., Eds.; The Humana Press: Totowa, NJ, 2004; pp 37–64.
- (43) Wang, Q.; Zhang, Y.; Hall, J. P.; Lin, L.-L.; Raut, U.; Mollova, N.; Green, N.; Cuzzo, J.; Chesley, S.; Xu, X.; Levin, J. I.; Patel, V. S. A rat pharmacokinetic/pharmacodynamic model for assessment of lipopolysaccharide-induced tumor necrosis factor- α production. *J. Pharmacol. Toxicol. Methods* **2007**, *56*, 67–71.

JM070436Q